Ministry of Education of Russian Federation

Novosibirsk State University

Department of Mechanics and Mathematics

Chair of Mathematical Methods in Geophysics

Master of Science Thesis

Milana A. AIZENBERG

Research of properties of reflection and transmission operators in the transmission problem at interface between two homogeneous half-spaces

Scientific supervisors:

Professor Kamill D. Klem-Musatov

Doctor Vladimir A. Tcheverda

Novosibirsk, 2003

CONTENTS

Introduction 3

1. Reflection and transmission operators in the transmission problem for acoustic waves . .5
   1.1. Statement of the canonical problem 7
   1.2. Space source field 7
   1.3. Space scattered field 8
   1.4. Transmission transform at interface of half-spaces 9
   1.5. Reflection and transmission operators 11
   1.6. Effective reflection and transmission coefficients 14

2. Transmission operator in the transmission problem for elastic waves 23
   2.1. Statement of the canonical problem 23
   2.2. Space source field 25
   2.3. Space scattered field 28
   2.4. Transmission transform at interface of half-spaces 29
   2.5. Transmission operator 30
   2.6. Effective reflection and transmission coefficients 34

3. Simulation of scattered fields using effective coefficients 39
   3.1. Scheme of modified acoustic version of Tip Wave Superposition Method . . .39
   3.2. Acoustic wave field, single scattered at curvilinear interface 41
   3.3. Elastic wave field, scattered at plane interface 52

Conclusions 57

References 58

INTRODUCTION

At present, one of the actual problems of seismics is to improve correctness of description of reflection and transmission processes at curvilinear interfaces in terms of surface integrals. Therefore in analytical and numerical methods for solving realistic inverse geophysical problems in composite media they use splitted interpretation algorithms [25, 39]. Such algorithms are oriented to the sequential reconstruction of the geometrical and physical parameters of the isolated and spatially localized elements of a complex medium. Within the bounds of such approach, the algorithms for restoration of the local heterogeneities [14, 34], the algorithms for restoration of the reflector form [17] and the algorithms for estimation of the reflection coefficient at a target interface [24] are intensively developing.

Because of new directions of research, there arises a problem of switching from using the plane-wave reflection and transmission coefficients to integral algorithms that allow more realistic description of multiple scattering processes. Most of the true migration algorithms are oriented to the integral Kirchhoff-type operators that construct reversed continuations of the wave fields. Existing reflection coefficient restoration algorithms use its rough approximation: the plane-wave reflection and transmission coefficients that do not allow taking into consideration influence of the incident wave front curvature and local heterogeneity of the medium.

To develop more accurate algorithms, it is desirable to obtain exact description of the reflection/transmission process in terms of integral operators. Numerous attempts were made to use strong statements of boundary problems of mathematical wave theory to construct such operators. By now, next results are achieved. In [42] the differential Ricatti-type equations for the reflection operators are obtained. In [22] the integral equations for reflection and transmission operators are obtained and for the case of plane interface between homogeneous half-spaces their explicit form is obtained. In [29] they obtained analogous integral equations for elastic reflection and transmission operators. For the case of homogeneous media, in [38, 41] they give heuristic approach for construction such operators, which is based on decomposition of Green functions in Helmholtz integral over system of plane waves.

The long standing joint research on the mathematical simulation of the wave fields in a stratified inhomogeneous medium was carried out by the researchers K.D. Klem-Musatov and A.M. Aizenberg from Institute of Geophysics SB RAS and H.B. Helle and J. Pajchel from the Research Center of Norsk Hydro (Bergen, Norway). They worked out the algorithms of the Tip Wave Superposition Method for implementation in the inverse problem algorithms restoring the reflecting and scattering properties of the local elements of the target interface [11, 32]. Since in these algorithms they also used the plane-wave reflection and transmission coefficients as an approximation of the reflection and transmission operators, the wave fields contained artefacts, which were generated by critical points of the plane-wave reflection and transmission coefficients. Such artefacts have wave properties, therefore it is difficult to interpret the wave picture. To remove artefacts, it is necessary to construct exact description of the reflection and transmission operators at a separate curvilinear interface. Within the bounds of initiative project “Development of theory of seismic wave propagation and diffraction” (supervisor K.D. Klem-Musatov, RFBR grants 97-05-65197 and 00-05-65397) they developed a modified system of boundary integral equations for the Cauchy data (limit values of the wave fields) at curvilinear interface between heterogeneous acoustic media, which contains unknown earlier exact integral reflection and transmission operators [31]. Within the bounds

of the project of RFBR grant 03-05-64941 they continue the research on generalization this theory for the case of elastic waves.

Starting from September 2000, this research has been implemented in Institute of Geophysics SB RAS as a part of above-mentioned RFBR projects and was supported by RFBR grant for young scientists 02-05-06136. Numerical experiments on simulation of scalar wave fields were made during summer practice of the author in the Research Centre of Norsk Hydro (Bergen, Norway) in August-September 2002 [10]. In this thesis we derive unknown earlier integral reflection and transmission operators for plane interface between homogeneous elastic media. Their form is similar to common reflection and transmission operators for acoustic waves [31]. To make analysis of new operators easier, we give derivation and analysis of such operators for both acoustic and elastic waves. The subject of investigation is reflection and transmission operators for acoustic and elastic waves. Basic results of the thesis are: 1) representation of operators in the form of effective (functional) coefficients; 2) universal algorithm of their numerical realization; 3) improving correctness of simulation of single scattered wave fields in the vicinity of critical ray and overcritical zone when using the effective reflection coefficient.

Basic results of the research are represented at International Scientific Conference for Students "Student and Scientific-Technical Progress" (Novosibirsk, 2001, 2002, 2003) on the section Mathematics (subsection Differential equations) and section Geology (subsection Geophysics), International Conference for Young Scientists, Specialists and Students "Geophysics 2001" (Novosibirsk, 2001), International Conference "Acoustics of Inhomogeneous Media V" (Novosibirsk, 2002), 5th International Conference for Young Scientists on Mathematical Modeling and Data Technologies (Novosibirsk, 2002), seminar of the Research Centre of Norsk Hydro (Bergen, Norway, 2002) and Scientific Council of Institute of Geophysics SB RAS (Novosibirsk, 2003). Basic results are published in [1-9].

Thesis consists of Introduction, three Sections and Conclusions. In Section 1 we give analytical properties of the reflection and transmission operators for acoustic waves, introduce corresponding effective coefficients and give their properties. In Section 2 we give analytical properties of matrix transmission operator for elastic waves, derive matrices of effective reflection and transmission coefficients and give their properties. In Section 3 we give examples of using effective coefficients for simulation of scattered fields in acoustic and elastic cases. In Conclusions we give basic results of the research, estimate their novelty and contribution of the author, explain possible domains of usage of effective reflection and transmission coefficients.

1. REFLECTION AND TRANSMISSION OPERATORS IN THE TRANSMISSION PROBLEM FOR ACOUSTIC WAVES

In this Section we discuss analytical properties of the reflection and transmission operators for acoustic waves, derive corresponding effective coefficients and bring their properties. In Subsection 1.1 we introduce exact statement on the canonical transmission problem, which describes scattering of stationary acoustic waves at infinite plane interface of two homogeneous half-spaces. In Subsection 1.2 solution of the problem is represented as sum of unknown source field as volume integral and unknown scattered field. In Subsection 1.3 the space scattered field is introduced as result of action of the Weyl-type propagation operator over unknown scattered field trace at the interface. In Subsection 1.4 we introduce transmission transform that transforms source field trace into scattered field trace and has form of matrix transmission operator. Analytical properties of the transmission operator are analyzed. Its scalar elements, which are represented by reflection and transmission operators of convolution type, are introduced through the Fourier transform in the domain of space frequencies and classical plane-wave reflection and transmission coefficients (Fresnel coefficients). In Subsection 1.5 we discuss properties of the convolution kernel and give figures of real and imaginary parts of the kernel for arbitrary velocity contrasts. In Subsection 1.6 action of the reflection and transmission operators over the source field trace is reduced to the pointwise multiplication with the corresponding effective coefficients. It is shown that effective coefficients tend to corresponding plane-wave coefficients when angular frequency tends to infinity. Pictures of the effective reflection coefficient for various density contrasts are brought.

1.1. Statement of the canonical problem

By a transmission problem it is usual to mean wave scattering by an infinite curvilinear interface Σ between two inhomogeneous half-spaces $\Omega_j \subset \mathrm{R}^3$, $j=1,2$. Let $H^2_{-\eta}(\Omega_j)=\left\{u\in H^2(\Omega_j\cap B_{Rj}),\forall R>0 \,\middle|\, (1+|\mathrm{x}|)^{-\eta}\,\partial^\alpha u\in L_2(\Omega_j),|\alpha|\le 2\right\}$ be the weighted Sobolev space, and $B^*(\Omega_j)$ be denotation of the Besov space, which is a class of elements u belonging to $L_2(\Omega_j\cap B_{Rj}),\forall R>0$ and satisfying relation $\|u\|^2_{B^*(\Omega_j)}=\sup\limits_{R>1}\dfrac{1}{R}\iiint\limits_{|\mathrm{x}|<R,\ \mathrm{x}\in\Omega_j}|u|^2\,d\mathrm{x}<\infty$, where $B_{Rj}=\left\{\mathrm{x}\in\Omega_j \,\middle|\, |\mathrm{x}|<R\right\}$. In [37, 43] it was shown that the unique solution of this problem for scalar waves exists in the class of functions $H^2_{-\eta}(\Omega_j)\cap B^*(\Omega_j)$, $\eta>1/2$.

In this Subsection we consider canonical medium model: plane interface Σ divides two homogeneous half-spaces Ω_1 and Ω_2 (Fig. 1.1). Let $\mathrm{x}=(\overline{\mathrm{x}},x_3)\in\mathrm{R}^3$ be system of Cartesian coordinates, where $\overline{\mathrm{x}}=(x_1,x_2)\in\Sigma$ and the axis x_3 is directed into Ω_1. Introduce denotation for limit points $\overline{\mathrm{x}}_j=(\overline{\mathrm{x}},\varepsilon_j 0)\in\Omega_j$, $\varepsilon_j=(-1)^{j-1}$.

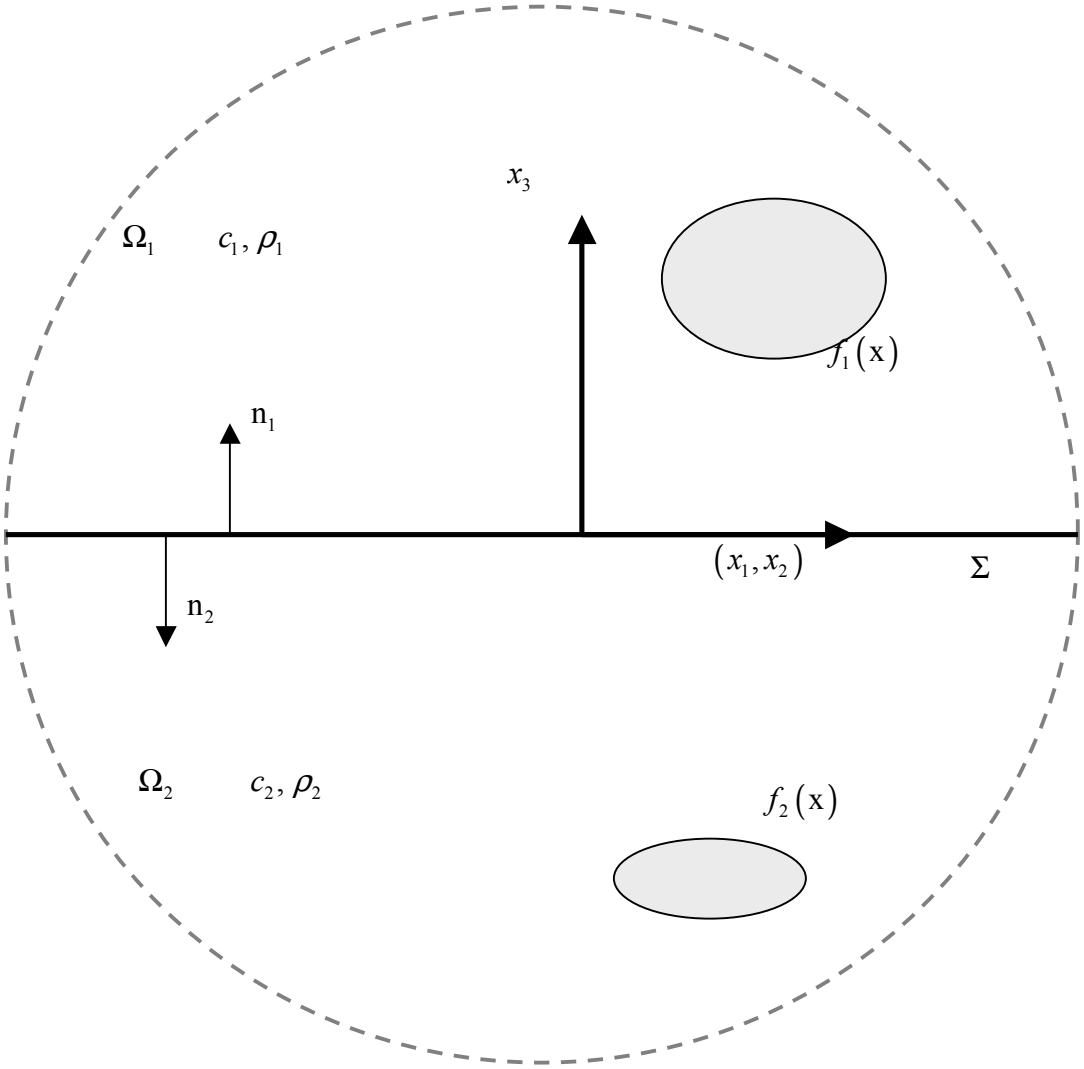


Fig. 1.1. Medium model.

For such medium model, the transmission problem can be reduced to determination of two complete wave fields $u_1(\mathrm{x})$ and $u_2(\mathrm{x})$. Each field $u_j(\mathrm{x}) \in H^2_{-\eta}(\Omega_j) \cap B^*(\Omega_j)$ satisfies the stationary wave equation

$$\left(\Delta + k_j^2\right) u_j(\mathrm{x}) = -f_j(\mathrm{x}-\mathrm{z}_j), \quad \mathrm{x} \in \Omega_j, \tag{1.1}$$

where $k_j = \omega / c_j$ is the wave number, ω is the angular frequency, c_j is constant wave propagation velocity in Ω_j, and the radiation condition at infinity in Ω_j is

$$\lim_{R\to\infty} \frac{1}{R} \iiint\limits_{\mathrm{x}\in\Omega_j,\,|\mathrm{x}|<R} \left|\mathrm{x}\cdot\nabla u_j / |\mathrm{x}| - ik_j u_j\right|^2 d\mathrm{x} = 0 \tag{1.2}$$

Let us assume that the volume density of sources $f_j(\mathrm{x}-\mathrm{z}_j)$ is given in the domain $\operatorname{supp} f_j \subset \Omega_j$, where z_j is an arbitrary point with fixed position inside $\operatorname{supp} f_j$.

Pair of complete wave fields $u_1(\mathrm{x})$ and $u_2(\mathrm{x})$ satisfy the transmission conditions at the interface Σ

$$u_1(\overline{\mathrm{x}}_1) = u_2(\overline{\mathrm{x}}_2), \quad \partial_3 u_1(\overline{\mathrm{x}}_1) = \beta\, \partial_3 u_2(\overline{\mathrm{x}}_2), \tag{1.3}$$

where $\beta = \rho_1/\rho_2$ is the given constant coefficient, ρ_j is the medium density in Ω_j, $\partial_3 = \partial/\partial x_3$ is the normal derivative to the interface.

1.2. Space source field

Represent solution of the problem (1.1)-(1.3) in the form of sum

$$u_j(\mathrm{x}) = u_j^-(\mathrm{x}) + u_j^+(\mathrm{x}), \tag{1.4}$$

where $u_j^-(\mathrm{x})$ is the given partial solution of the problem (1.1)-(1.2), $u_j^+(\mathrm{x})$ is the scattered field, which is solution of the problem (1.1)-(1.3) with the homogeneous equation (1.1).

Partial solution $u_j^-(\mathrm{x})$ can be introduced by the volume integral [35]

$$u_j^-(\mathrm{x}) = \iiint\limits_{\operatorname{supp} f_j} g_j(\mathrm{x},\mathrm{x}')\, f_j(\mathrm{x}'-\mathrm{z}_j)\, d\mathrm{x}' \tag{1.5}$$

and represents the source field, if the fundamental solution $g_j(\mathrm{x},\mathrm{x}')$ of the problem (1.1)-(1.2) has the form of spherical wave [40]

$$g_j(\mathrm{x},\mathrm{x}') = \exp\left(ik_j|\mathrm{x}-\mathrm{x}'|\right)/\left(4\pi|\mathrm{x}-\mathrm{x}'|\right) \tag{1.6}$$

Introduce operator of the twofold Fourier transform F by the formulas

$$\begin{aligned}\varphi(\overline{\mathrm{x}},x_3) = F\hat{\varphi}(\zeta,x_3) &= \frac{1}{2\pi}\iint\limits_{\mathrm{R}^2}\hat{\varphi}(\zeta,x_3)\exp\left(i\zeta\overline{\mathrm{x}}\right)d\zeta,\\ \hat{\varphi}(\zeta,x_3) = F^{-1}\varphi(\overline{\mathrm{x}},x_3) &= \frac{1}{2\pi}\iint\limits_{\mathrm{R}^2}\varphi(\overline{\mathrm{x}},x_3)\exp\left(-i\zeta\overline{\mathrm{x}}\right)d\overline{\mathrm{x}}\end{aligned} \tag{1.7}$$

with the Weyl transform $\hat{E}_j^{\pm}(\zeta,x_3) = \exp\left(\pm i\varepsilon_j\zeta_{3j}x_3\right)$ and arithmetical square root $\zeta_{3j} = \sqrt{k_j^2-\zeta^2}$, $\zeta = |\zeta|$ [23]. Further, we will omit the argument ζ to simplify notations.

Introduce spectral representation of the source field (1.5). For that, let us represent the fundamental solution (1.6) when $\mathrm{x}\in\mathrm{R}^3\setminus\overline{\Omega}_j$ in the form of the Weyl representation over the complete system of plane incoming waves

$$g_j(\mathrm{x};\mathrm{x}') = F\left[i\left(4\pi\,\zeta_{3j}\right)^{-1}\hat{E}_j^-(x_3-x_3')\exp\left(-i\zeta\overline{\mathrm{x}}'\right)\right] \tag{1.8}$$

Substituting (1.8) in (1.5), we obtain the source field (1.5) in the form of Weyl representation

$$u_j^-(\mathrm{x}) = F\left[\hat{u}_j^-\,\hat{E}_j^-(x_3)\right], \tag{1.9}$$

where

$$\hat{u}_j^- = i\left(4\pi\,\zeta_{3j}\right)^{-1}\iiint\limits_{\operatorname{supp}\varphi_j}\hat{E}_j^-(-x_3')\exp\left(-i\zeta\overline{\mathrm{x}}'\right)f_j\left(\mathrm{x}'-\mathrm{z}_j\right)d\mathrm{x}' \tag{1.10}$$

In particular, when $\mathrm{x}\to\overline{\mathrm{x}}_j$ in (1.9), we obtain the source field trace at the interface

$$u_j^-\left(\overline{\mathrm{x}}_j\right) = F\,\hat{u}_j^- \tag{1.11}$$

1.3. Space scattered field

Introduce spectral representation of the scattered field $u_j^+(\mathrm{x})$ when $\mathrm{x}\in\Omega_j$ in the form of Weyl representation over the complete system of outgoing plane-waves

$$u_j^+(\mathrm{x}) = F\left[\hat{u}_j^+\,\hat{E}_j^+(x_3)\right] \tag{1.12}$$

In the limiting case $\mathrm{x} \to \overline{\mathrm{x}}_j$ the formula (1.12) gives the scattered field trace at interface

$$u_j^+\left(\overline{\mathrm{x}}_j\right) = F\, u_j^+ \tag{1.13}$$

From (1.13) it follows

$$\hat{u}_j^+ = F^{-1}\, u_j^+\left(\overline{\mathrm{x}}_j\right) \tag{1.14}$$

Substitution of relation (1.14) into representation (1.12) gives desired form of the space scattered wave field

$$u_j^+(\mathrm{x}) = F\left[\hat{E}_j^+(x_3)\, F^{-1}\, u_j^+\left(\overline{\mathrm{x}}_j\right)\right] \tag{1.15}$$

In spite of the formula (1.15) defines solution (1.4) when the source field (1.5) is given, the scattered field trace $u_j^+\left(\overline{\mathrm{x}}_j\right)$ still remains unknown.

From the relation (1.15) it follows that operator $F\,\hat{E}_j^+(x_3)\,F^{-1}$, which transforms the trace $u_j^+\left(\overline{\mathrm{x}}_j\right)$ into the space scattered field $u_j^+(\mathrm{x})$, is a propagation operator. This operator may also be introduced with help of double layer potential.

1.4. Transmission transform at interface of half-spaces

Let us determine dependence between pair of unknown traces (1.13) and pair of given source field traces (1.11) with help of the transmission conditions (1.3). Consider spectral form. Let us substitute representation (1.4) into the transmission conditions (1.3) and apply operator F^{-1} to both equalities. As a result we obtain spectral form of the transmission conditions

$$\begin{aligned} &\hat{u}_1^- + \hat{u}_1^+ = \hat{u}_2^- + \hat{u}_2^+, \\ &\hat{u}_1'^- + \hat{u}_1'^+ = \beta\left(\hat{u}_2'^- + \hat{u}_2'^+\right), \end{aligned} \tag{1.16}$$

where $\hat{u}_j'^+ = F^{-1}\,\partial_3 \hat{u}_j^+\left(\overline{\mathrm{x}}_j\right)$ and $\hat{u}_j'^- = F^{-1}\,\partial_3 \hat{u}_j^-\left(\overline{\mathrm{x}}_j\right)$.

System (1.16), which consists of two equations, contains four unknown spectra $\hat{u}_j^+$ and $\hat{u}_j'^+$. It is necessary to add two linearly independent relations, which are based on properties of solutions of the problem (1.1)-(1.2) and are not connected with the transmission conditions (1.3). To obtain such additional relations, let us prove next lemma.

Lemma 1. The impedance type relations hold true

$$\hat{u}_j'^+ = i\,\varepsilon_j \zeta_{3j} \hat{u}_j^+, \quad \hat{u}_j'^- = -i\,\varepsilon_j \zeta_{3j} \hat{u}_j^- \tag{1.17}$$

Proof. Differentiate representations (1.12) and (1.9) in the line x_3, let $\mathrm{x} \to \overline{\mathrm{x}}_j$ and apply operator F^{-1} to obtained equalities. As a result we obtain desired impedance relations. *Lemma is proven.*

Inspite of the fact that the system (1.16)-(1.17) contains six relations for four unknown quantities, it is compatible by definition. Substituting impedance relations (1.17) into conditions (1.16), we reduce the system (1.16)-(1.17) to the system of two linearly independent equations for two unknown quantities $\hat{u}_j^+$. Represent its solution in the matrix form

$$\hat{\mathrm{u}}^+ = \hat{\mathrm{K}}\, \hat{\mathrm{u}}^-, \tag{1.18}$$

with spectral vectors

$$\hat{\mathrm{u}}^\pm = \left(\hat{u}_1^\pm, \hat{u}_2^\pm\right) \tag{1.19}$$

and a spectral matrix

$$\hat{\mathrm{K}} = \begin{bmatrix} \hat{k}_{11} & \hat{k}_{12} \\ \hat{k}_{21} & \hat{k}_{22} \end{bmatrix} \tag{1.20}$$

The elements of the matrix (1.20) are reflection $\hat{k}_{11}, \hat{k}_{22}$ and transmission $\hat{k}_{12}, \hat{k}_{21}$ coefficients for plane waves (Fresnel coefficients) [18] given by the formulas

$$\hat{k}_{11} = \frac{\zeta_{31} - \beta\zeta_{32}}{\zeta_{31} + \beta\zeta_{32}}, \quad \hat{k}_{12} = 1 - \hat{k}_{11}, \quad \hat{k}_{21} = 1 + \hat{k}_{11}, \quad \hat{k}_{22} = -\hat{k}_{11} \tag{1.21}$$

Introduce vectors of the scattered field traces and source field traces at the interface

$$\mathrm{u}^\pm = \left(u_1^\pm, u_2^\pm\right) \tag{1.22}$$

and a matrix operator

$$\mathrm{F} = \begin{bmatrix} F & 0 \\ 0 & F \end{bmatrix} \tag{1.23}$$

Applying the operator (1.23) to the equality (1.18) and letting $\hat{\mathrm{u}}^- = \mathrm{F}^{-1}\mathrm{u}^-$ in its right part, we obtain a transmission transform at the interface

$$\mathrm{u}^+ = \mathrm{K}\, \mathrm{u}^-, \tag{1.24}$$

where the matrix transmission operator has the form

$$\mathrm{K} = \begin{bmatrix} K_{11} & K_{12} \\ K_{21} & K_{22} \end{bmatrix} \tag{1.25}$$

K_{mn} are reflection operators (when $m = n$) and transmission operators (when $m \neq n$), which according to formulas (1.20) have the form

$$K_{mn} = F\, \hat{k}_{mn}\, F^{-1} \tag{1.26}$$

The transmission operator (1.25) is a particular case of the more common transmission operator obtained in [31].

Let us note some mathematical properties of the operator (1.25). Letting in (1.4) $\mathrm{x} \to \overline{\mathrm{x}}_j$, introduce vector of the interference field traces $\mathrm{u} = \mathrm{u}^- + \mathrm{u}^+$. Then the next lemma holds true.

Lemma 2. Vector u is the fixed point of the transmission operator K.

Proof. From the definitions (1.21) it trivially follows that $\mathrm{K}^2 = \mathrm{I}$. Taking into consideration this property and applying K on the relation (1.24) from the left, we obtain $\mathrm{u}^- = \mathrm{K}\,\mathrm{u}^+$. Summarizing this relation with (1.24), we obtain the identity $\mathrm{u} = \mathrm{K}\,\mathrm{u}$, which shows that the vector of the interference field traces f is the fixed point of the operator K. *Lemma is proven.*

1.5. Reflection and transmission operators

By virtue of the definitions (1.21), the transmission operators may be represented as

$$K_{(3-j)j} = I + K_{jj}, \tag{1.27}$$

where I is the operator which acts by the rule $u_j^-\left(\overline{\mathrm{x}}_j\right) = I\left(\overline{\mathrm{x}}_j, \cdot\right) u_j^-\left(\cdot\right)$. Based on the representation (1.27), we will consider only reflection operators K_{jj}. Represent these operators in the form

$$K_{jj} = \varepsilon_j \left(\frac{1-\beta}{1+\beta} I + Q \right), \tag{1.28}$$

where

$$Q = F\, \hat{q}\left(\eta; \mathrm{p}\right) F^{-1}, \tag{1.29}$$

$$\hat{q}\left(\eta; \mathrm{p}\right) = \frac{\sqrt{\cos^2\psi - \eta^2} - \beta\sqrt{\sin^2\psi - \eta^2}}{\sqrt{\cos^2\psi - \eta^2} + \beta\sqrt{\sin^2\psi - \eta^2}} - \frac{1-\beta}{1+\beta}, \tag{1.30}$$

$\eta = \zeta / k$ is a dimensionless variable, $k = \sqrt{k_1^2 + k_2^2}$ is a mean-square wave number for acoustic interface, $\mathrm{p} = (\psi, \beta)$ is a vector of the model parameters, $\psi = \operatorname{arctg}(k_2 / k_1) = \operatorname{arctg}(c_1 / c_2)$. From the definition of the coefficient (1.30) it trivially follows

$$\hat{q}(\eta; \mathrm{p}) = -\hat{q}(\eta; \mathrm{p}'), \quad \mathrm{p}' = \left(\pi/2 - \psi, \beta^{-1}\right) \tag{1.31}$$

Therefore we will assume that the function (1.30) varies on the parametric set $\mathrm{p} \in [0, \pi/2] \times (0, 1]$.

Note that, by definition, the operator (1.29) has an equivalent convolution form $Q = q *$ with the kernel $q = (2\pi)^{-1} F \hat{q}$, which varies on the set $\mathrm{p} \in [0, \pi/2] \times (0, 1]$. From the formal standpoint, these two representation forms are equal. However, for the numerical realization the convolution form is preferable because of the next reasons. Disadvantage of the spectral form of the operator (1.29) appears in practical problems where the trace $u_j^-(\overline{\mathrm{x}}_j)$ is given as a mesh function with a grid step defined by experimental data. At the same time realization of the spectral representation of the operator (1.29) brings essential inaccuracies in denumerable trace of the scattered field. Advantage of the convolution form consists in the fact that the kernel q, based on symmetry of the coefficient (1.30) on ζ-plane, may be represented as one-dimensional integral and tabulated on the set $\mathrm{p} \in [0, \pi/2] \times (0, 1]$.

If we permute the operators F and F^{-1} in (1.29), the action of the operator (1.29) over the trace $u_j^-(\overline{\mathrm{x}}_j)$ may be written as a two-dimensional convolution

$$Q\, u_j^-(\overline{\mathrm{x}}_j) = \iint_{\mathrm{R}^2} q(k\overline{\mathrm{y}}; \mathrm{p})\, u_j^-(\overline{\mathrm{x}}_j - \overline{\mathrm{y}}_j)\, d(k\overline{\mathrm{y}}) \tag{1.32}$$

with a dimensionless kernel

$$q(k\overline{\mathrm{y}}; \mathrm{p}) = \frac{1}{2\pi} \iint_{\mathrm{R}^2} \hat{q}(\eta; \mathrm{p}) \exp(i\eta k\overline{\mathrm{y}})\, d\eta \tag{1.33}$$

and a dimensionless vector $\eta = \zeta / k$. Since the coefficient (1.30) has the order of decreasing $\mathrm{O}(\eta^{-2})$ at infinity, the integral (1.33) converges in the classical meaning and does not contain generalized functions.

It is easy to show that in vicinity of singular points $\eta = \cos\psi$ and $\eta = \sin\psi$ function $\hat{q}$ belongs to the Hölder class $C^{1/2}$ with respect to the variable η [15]. Therefore the integral (1.33) exists only in terms of principal value and integration in (1.33) should be realized using spherical or rectangular method [28]. Taking into account the polar symmetry of the coefficient $\hat{q}$, it is naturally to choose the spherical method of integration. In two-dimensional case this corresponds to transferring to the polar coordinate systems (r, θ) at the interface

$$\overline{\mathrm{y}} = r\,\mathbf{i}, \quad \mathbf{i} = (\cos\theta, \sin\theta) \tag{1.34}$$

and (ζ, τ) at the plane of space frequencies

$$\zeta = \zeta\,\mathbf{j}, \quad \mathbf{j} = (\cos\tau, \sin\tau) \tag{1.35}$$

Letting the parameter k be fixed, introduce also dimensionless variables

$$\rho = kr, \quad \eta = \zeta / k \tag{1.36}$$

and definition of the Bessel function in the notations (1.36) by the formula [26]

$$J_0(\rho\eta) = \frac{1}{2\pi}\int_0^{2\pi} \exp\left[i\rho\eta\cos(\tau-\theta)\right] d\tau \tag{1.37}$$

Taking into consideration the formulas (1.34)-(1.37), the dimensionless kernel (1.33) can be represented as the direct Bessel transform of the zero order

$$q(\rho;\mathrm{p}) = \int_0^{\infty} \hat{q}(\eta;\mathrm{p}) J_0(\rho\eta)\,\eta\, d\eta \tag{1.38}$$

Notice that the improper integral (1.38) depends on the parameter ρ, which may take the value $\rho = 0$. We assume that the integral (1.38) is a continuous function of the variable ρ when $\rho \in (0,\infty)$ and $q(0;\mathrm{p}) = \lim_{r\to 0} q(\rho;\mathrm{p})$. To justify the continuity of the function (1.38) let us prove the next lemma.

Lemma 3. The integral (1.38) uniformly converges on the parametrical set $\Pi = \{\rho \in (0,\infty), \mathrm{p} \in [0,\pi/2]\times(0,1]\}$.

Proof. Rewrite the integral (1.38) in the form of sum

$$q(\rho;\mathrm{p}) = q_{(0,\eta_0)}(\rho;\mathrm{p}) + q_{(\eta_0,\infty)}(\rho;\mathrm{p}),$$

where η_0 is an arbitrary fixed number, $\eta_0 > \rho$, and

$$q_{(A,B)}(\rho;\mathrm{p}) = \int_A^B \hat{q}(\eta;\mathrm{p}) J_0(\rho\eta)\,\eta\, d\eta$$

Notice that in this form only integral $q_{(\eta_0,\infty)}(\rho;\mathrm{p})$ is improper. Because of this reason, further study reduces to its uniform convergence. For enough big η_0 and $\eta \in [\eta_0,\infty)$, the coefficient (1.30) allows expansion to the asymptotic series

$$\hat{q}(\eta;\mathrm{p}) = -\frac{\beta\cos 2\psi}{(1+\beta)^2}\eta^{-2} + \mathrm{O}\left(\eta^{-4}\right)$$

Therefore the function $\eta\,\hat{q}(\eta;\mathrm{p})$ on the set Π does not increase on the interval $\eta \in [\eta_0,\infty)$ and uniformly converges with respect to all parameters to zero with $\eta \to \infty$. At the same time, with regard to the Bessel function properties, for all $\rho \in (0,\infty)$ and $\eta \in [\eta_0,\infty)$ the relation holds true

$$\left|\int_{\eta_0}^{\eta} J_0(\rho\eta)\,d\eta\right| \le const$$

Then by virtue of the Dirichlet criterion [33] the integral $q_{(\eta_0,\infty)}(\rho;\mathrm{p})$ uniformly converges on the parametrical set Π. *Lemma is proven.*

Since the integral (1.38) can not be computed in an explicit form, it is necessary to estimate the order of its decreasing at infinity. To obtain such estimation we carried out series of the numerical experiments for wide enough range of varying of the main parameters. Tests show that the kernel (1.38) has asymptotic behavior at infinity

$$q(\rho;\mathrm{p}) = \mathrm{P}(\rho;\mathrm{p})\,\rho^{-3/2},$$

where the non-decreasing oscillating function $\mathrm{P}(\rho;\mathrm{p})$ is bounded in absolute value by some function of parameters.

For computation of the Bessel transform (1.38), we used the Newton-Cotes scheme (of closed type) 26.4.16 from [26]. To make numerical integration stable, we applied combination of method of integration by parts in neighborhood of critical points and method of adaptive grids. Real and imaginary parts of the kernel $q(\rho;\mathrm{p})$ with $\beta = 1$ and $\mathrm{tg}\,\psi \in (0.2, 0.8)$ are shown at Fig. 1.2.

1.6. Effective reflection and transmission coefficients

Since in applied problems of acoustics they multiply the source field traces by the plane-wave coefficients to describe the reflection and transmission processes at interface, we rewrite the transmission transform (1.24) in the form of pointwise multiplication. To give the convolution (1.32) this form, it is necessary to represent operators (1.28) in the form

$$K_{jj} = \varepsilon_j\left(\frac{1-\beta}{1+\beta} + \xi_j\right)I \qquad (1.39)$$

To define the coefficients ξ_j, let us prove the auxiliary lemma.

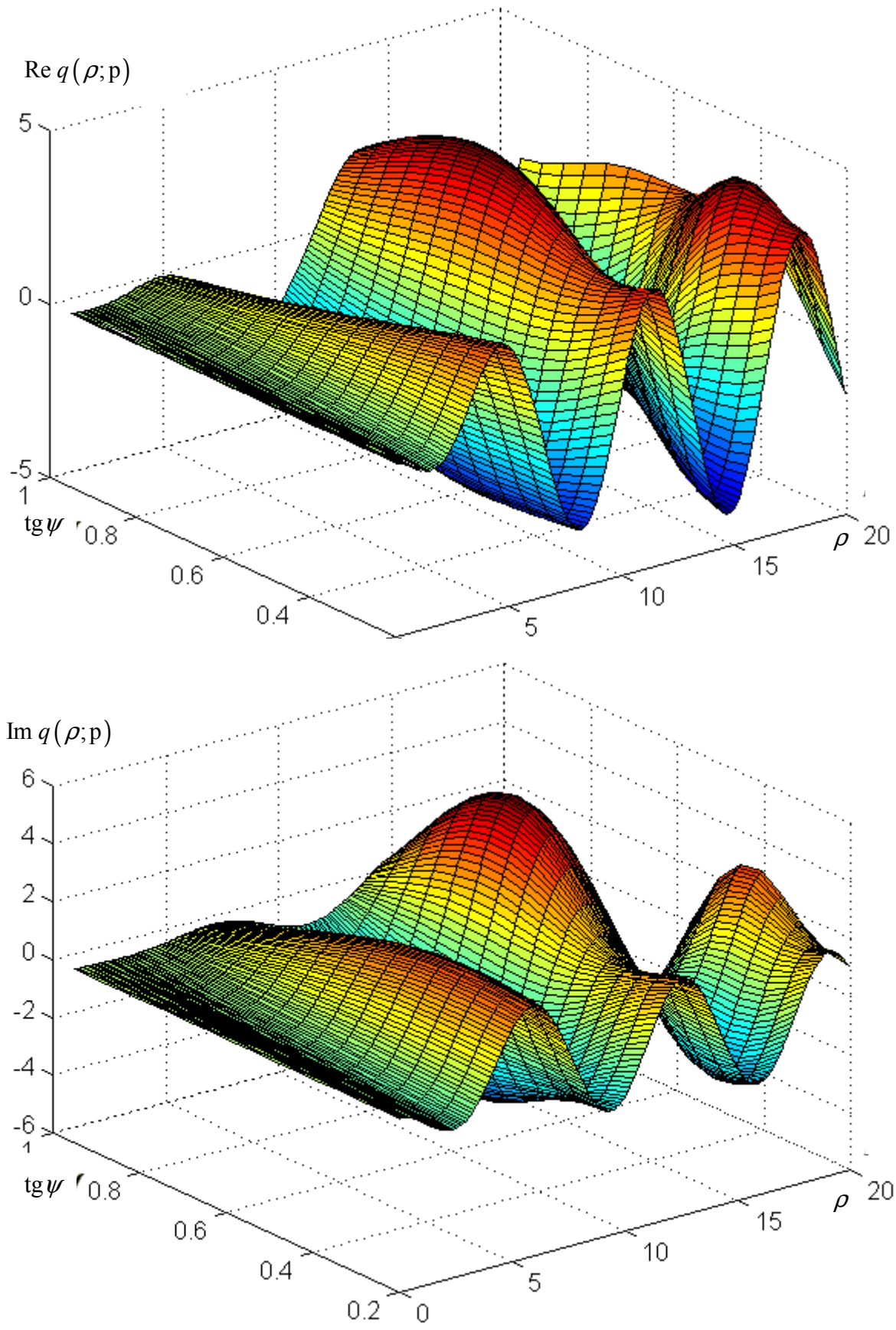


Fig. 1.2. Real and imaginary parts of the kernel.

Lemma 4. The trace $u_j^-\left(\overline{\mathrm{x}}_j\right)$ can be represented in the form

$$u_j^-\left(\overline{\mathrm{x}}_j\right) = k\, L_j\left(kR_j, \mathrm{v}_j, \psi\right),$$

where $L_j\left(kR_j, \mathrm{v}_j, \psi\right)$ is a function which depends only on the dimensionless arguments $R_j = \left|\overline{\mathrm{x}}_j - \mathrm{z}_j\right|$, $\mathrm{v}_j = \left(\gamma_j, \delta_j, kl_j\right)$ is a parametrical vector, γ_j and δ_j are polar and latitudinal angles of the spherical coordinate system with the center at the point z_j, l_j is a specific linear size of the support $\operatorname{supp}\varphi_j$.

Proof. Introduce change of variables $\mathrm{y} = \mathrm{x}' - \mathrm{z}_j$ in (1.10) and substitute the stating to (1.10). We obtain the trace in the form

$$u_j^-\left(\overline{\mathrm{x}}_j\right) = \frac{i}{8\pi^2}\iint\limits_{\mathrm{R}^2} \frac{\hat{\Phi}_j\left(\zeta/k, kl_j, \psi\right)}{\zeta_{3j}}\hat{E}_j^-\left(-z_{3j}\right)\exp\left[i\zeta\left(\overline{\mathrm{x}} - \overline{\mathrm{z}}_j\right)\right]d\zeta,$$

where

$$\hat{\Phi}_j\left(\zeta/k, kl_j, \psi\right) = \iiint\limits_{\operatorname{supp}\varphi_j} \hat{E}_j^-\left(-y_3\right)\exp\left(-i\zeta\overline{\mathrm{y}}\right) f_j\left(\mathrm{y}\right) d\mathrm{y}$$

is a dimensionless function. Introducing a dimensionless vector $\eta = \zeta/k$, in the integral representation of the trace, we obtain the desired relation, where

$$L_j\left(kR_j, \mathrm{v}_j, \psi\right) = \frac{i}{8\pi^2}\iint\limits_{\mathrm{R}^2} \frac{\hat{\Phi}_j\left(\eta, kl_j, \psi\right)}{\sqrt{\left(k_j/k\right)^2 - \eta^2}}\exp\left[i\, kR_j \mathbf{i}_j \cdot \eta_j\right] d\eta,$$

$$\eta_j = \left(\eta, -\sqrt{\left(k_j/k\right)^2 - \eta^2}\right),$$

$k_1/k = \cos\psi$, $k_2/k = \sin\psi$. *Lemma is proven.*

Using Lemma 4, introduce the normalized source field trace by the formula

$$N_j\left(k\overline{\mathrm{y}}_j; kR_j, \mathrm{v}_j, \psi\right) = \frac{u_j^-\left(\overline{\mathrm{x}}_j - \overline{\mathrm{y}}_j\right)}{u_j^-\left(\overline{\mathrm{x}}_j\right)} \tag{1.40}$$

Taking into consideration the definition (1.40), the convolution (1.32) may be written in the variables (1.34) and (1.36) in the form of multiplication

$$Q\, u_j^-\left(\overline{\mathrm{x}}_j\right) = \xi_j\left(kR_j; \mathrm{v}_j, \mathrm{p}\right) u_j^-\left(\overline{\mathrm{x}}_j\right), \tag{1.41}$$

where the desired coefficient ξ_j is defined in the form of normalized convolution

$$\xi_j\left(kR_j;\mathrm{v}_j,\mathrm{p}\right)=\int_0^{\infty} q\left(\rho;\mathrm{p}\right) D_j\left(\rho;kR_j,\mathrm{v}_j,\psi\right)\rho\, d\rho\,, \tag{1.42}$$

with an integral of averaging of the normalized trace (1.40) over the polar angle

$$D_j\left(\rho;kR_j,\mathrm{v}_j,\psi\right)=\frac{1}{2\pi}\int_0^{2\pi} N_j\left(\rho\mathbf{i};kR_j,\mathrm{v}_j,\psi\right)d\theta \tag{1.43}$$

Taking into account (1.22), substitution of (1.39) and (1.27) into (1.24) gives representation of the scattered field traces as

$$u_j^{+}\left(\overline{\mathrm{x}}_j\right)=u_{j,r}^{+}\left(\overline{\mathrm{x}}_j\right)+u_{j,t}^{+}\left(\overline{\mathrm{x}}_j\right), \tag{1.44}$$

where the traces of reflected $u_{j,r}^{+}\left(\overline{\mathrm{x}}_j\right)$ and transmitted $u_{j,t}^{+}\left(\overline{\mathrm{x}}_j\right)$ fields have the form

$$u_{j,r}^{+}\left(\overline{\mathrm{x}}_j\right)=\chi_{jj}\, u_j^{-}\left(\overline{\mathrm{x}}_j\right),\quad u_{j,t}^{+}\left(\overline{\mathrm{x}}_j\right)=\chi_{j(3-j)}\, u_{3-j}^{-}\left(\overline{\mathrm{x}}_{3-j}\right), \tag{1.45}$$

and coefficients are given by the formulas

$$\begin{aligned}&\chi_{jj}\left(kR_j;\mathrm{v}_j,\mathrm{p}\right)=\varepsilon_j\left[\frac{1-\beta}{1+\beta}+\xi_j\left(kR_j;\mathrm{v}_j,\mathrm{p}\right)\right],\\ &\chi_{(3-j)j}\left(kR_j;\mathrm{v}_j,\mathrm{p}\right)=1+\chi_{jj}\left(kR_j;\mathrm{v}_j,\mathrm{p}\right)\end{aligned} \tag{1.46}$$

Although the formulas (1.45) have the form of linear transformation, they cannot be considered this way. The reason is the coefficients (1.46) are expressed through the normalized convolutions $\xi_j\left(kR_j;\mathrm{v}_j,\mathrm{p}\right)$, which depend on the distribution of the traces $u_j^{-}\left(\overline{\mathrm{x}}_j\right)$ over the interface. The scheme of action of the effective coefficients is shown on Fig. 1.3.

To validate the representation (1.45), let us consider the limiting case $kR_j\to\infty$ in coefficients (1.46). From the formulas (1.40), (1.42) and (1.43) it follows that it is enough to realize such limiting transfer immediately for each trace $u_j^{-}\left(\overline{\mathrm{x}}_j\right)$.

On the assumption $k=const$ and $R_j\to\infty$, the source field trace $u_j^{-}\left(\mathrm{x}\right)$ transfers to the plane wave with the wave vector $\mathrm{k}_j=k_j\,\mathbf{i}_j$, where $\mathbf{i}_j=\mathbf{i}_j\left(\overline{\mathrm{x}}_j\right)=\left(\sin\gamma_j\,\mathbf{e}_j,\cos\gamma_j\right)$ and $\mathbf{e}_j=\mathbf{e}_j\left(\overline{\mathrm{x}}_j\right)=\left(\cos\delta_j,\sin\delta_j\right)$. The source field trace $u_j^{-}\left(\overline{\mathrm{x}}_j\right)$ transfers to the plane wave trace

$$u_j^{-}\left(\overline{\mathrm{x}}_j\right)=\exp\left(i\,k\sigma_j\mathbf{e}_j\cdot\overline{\mathrm{x}}\right), \tag{1.47}$$

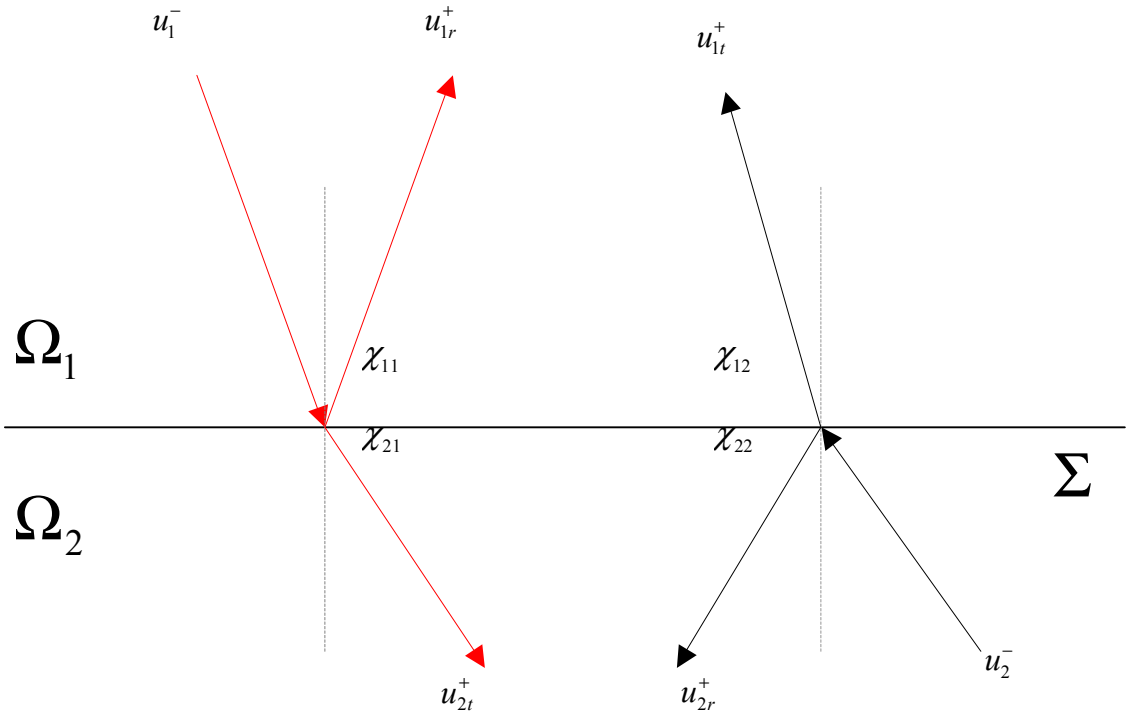


Fig. 1.3. Scheme of action of effective coefficients.

where $k\sigma_j$ is the module of the horizontal component of k_j, $\sigma_j = c_j \sin\gamma_j \left(c_1^{-2} + c_2^{-2}\right)^{-1/2}$. Introduce notation for the critical angle $\gamma_j^* = \arcsin\left(\min\left\{\mathrm{tg}\,\psi, \mathrm{ctg}\,\psi\right\}\right)$. In these assumptions, let us prove the next lemma.

Lemma 5. With $kR_j \to \infty$ and $\gamma_j \neq \gamma_j^*$ the coefficients (1.46) take the form

$$\chi_{jj}\left(\infty; \mathrm{v}_j, \mathrm{p}\right) = \varepsilon_j \frac{\sqrt{\cos^2\psi - \sigma_j^2} - \beta\sqrt{\sin^2\psi - \sigma_j^2}}{\sqrt{\cos^2\psi - \sigma_j^2} + \beta\sqrt{\sin^2\psi - \sigma_j^2}},$$
$$\chi_{(3-j)j}\left(\infty; \mathrm{v}_j, \mathrm{p}\right) = 1 + \chi_{jj}\left(\infty; \mathrm{v}_j, \mathrm{p}\right) \tag{1.48}$$

Proof. If we substitute the plane wave trace (1.47) to the definition (1.40), we obtain

$$N_j\left(\rho\mathbf{i}; \infty, \mathrm{v}_j, \psi\right) = \exp\left(-i\,\sigma_j \mathbf{e}_j \cdot \rho\mathbf{i}\right)$$

Hence, taking into consideration the Bessel transform definition and (1.43), we obtain a relation

$$D_j\left(\rho; \infty, \mathrm{v}_j, \psi\right) = J_0\left(\sigma_j \rho\right)$$

Substituting the last relation into (1.42) and using the definition of the inverse Bessel transform, we will obtain limiting value of the normalized convolution

$$\xi_j\left(\infty; \mathrm{v}_j, \mathrm{p}\right) = \int_0^\infty q\left(\rho; \mathrm{p}\right) J_0\left(\sigma_j \rho\right) \rho\, d\rho = \hat{q}\left(\sigma_j; \mathrm{p}\right)$$

Then from the relations (1.46) with $kR_j \to \infty$ we obtain the desired result. *Lemma is proven.*

From Lemma 5 it follows that the limiting values of coefficients (1.46) coincide with the plane wave reflection and transmission coefficients. Therefore coefficients (1.46) may be considered as effective reflection and transmission coefficients. From the formulas (1.48) it follows that plane-wave coefficients do not depend on frequency ω. This effect can be explained by the fact that the limiting case $kR_j \to \infty$ may be realized in two ways. The first technique was considered before.

The second technique of the realization of this limiting case corresponds to letting $k \to \infty$ with fixed R_j. Notice that the case $k \to \infty$ corresponds to switching form the exact description of the reflection/transmission phenomenon to the high-frequency asymptotic approximation. Therefore the formulas (1.44)-(1.45) together with coefficients (1.46) may be considered as theoretical explanation of the asymptotic ray theory assumption that for high frequencies arbitrary incident wave is reflected and transmitted as locally plane.

Below we give graphs of effective reflection coefficient $\chi_{11}(kR_1; \mathrm{v}_1, \mathrm{p})$ for the point source field. For comparison we give corresponding coefficient $\chi_{11}(\infty; \mathrm{v}_1, \mathrm{p})$ for the plane wave, which is tangent to the spherical wave at each point.

Computations are carried out for the medium model with typical for observed seismic waves velocities. The only one source of the spherical wave is situated in the point $\mathrm{z}_1 = (0, 0, h)$ of the half-space Ω_1 and generates the trace $u_1^-(\overline{\mathrm{x}}_1) = \exp(ik_1R_1)/(4\pi R_1)$ at the interface Σ. The parametrical vector is $\mathrm{v}_1 = (\gamma_1, 0, 0)$, where $\gamma_1 = \mathrm{arctg}(x_1/h)$. Modules of the source field $u_1^-(\overline{\mathrm{x}}_1)$ and corresponding reflected field $u_1^+(\overline{\mathrm{x}}_1)$ are shown on Fig. 1.4 (correspondingly). The medium model parameters are: $c_1 = 2\ km/s$, $c_2 = 4\ km/s$, $\beta = 1$, $\omega = 200\ Hz$, $h = 0.5\ km$.

Fig. 1.5 shows graphs of module of the effective reflection coefficient for various values of the parameter kh: $kh = 10^0$ (A), $kh = 10^1$ (B), $kh = 10^2$ (C), $kh = 10^6$ (D), $kh \to \infty$ (P). On figures the first graph corresponds to $\beta = 1$, i.e. to absence of the density contrast at the interface, the second graph corresponds to $\beta = 2$, i.e. to the absence of the acoustic resistance contrast since $\beta\ \mathrm{tg}\,\psi = 1$.

Graphs show that the effective reflection coefficient essentially depends on the dominant frequency and curvature of the wave front of the incident wave. This fact can be seen from deviation of the effective coefficient from the plane-wave coefficient in the pure reflection domain ($\gamma_1 < 30^0$). Notice that this deviation is stronger for small dominant frequencies. Oscillations of the effective coefficient in overcritical domain ($\gamma_1 > 30^0$) are generated by interference of reflected and head waves. For high frequencies the interference domain diminishes and, consequently, the head wave effect decreases. From graph it follows that, when frequency tends to infinity, the effective coefficient tends to the plane-wave coefficient. However, it remains to be smooth and differ from the plane-wave coefficient. Thus, if we multiply the source field trace by the effective coefficient, we keep smoothness of the scattered wave field.

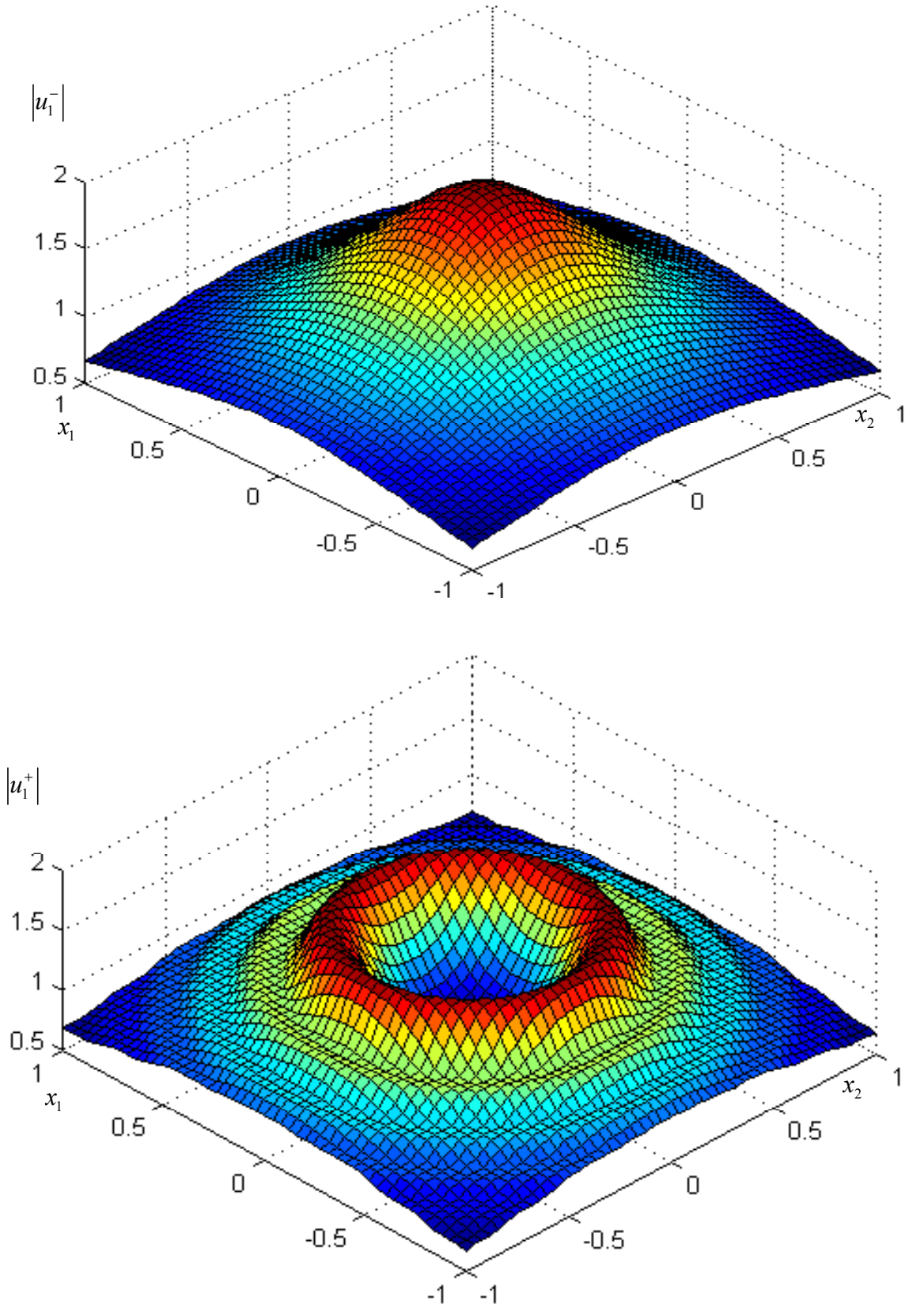


Fig. 1.4. Distribution of the source and reflected fields over the interface.

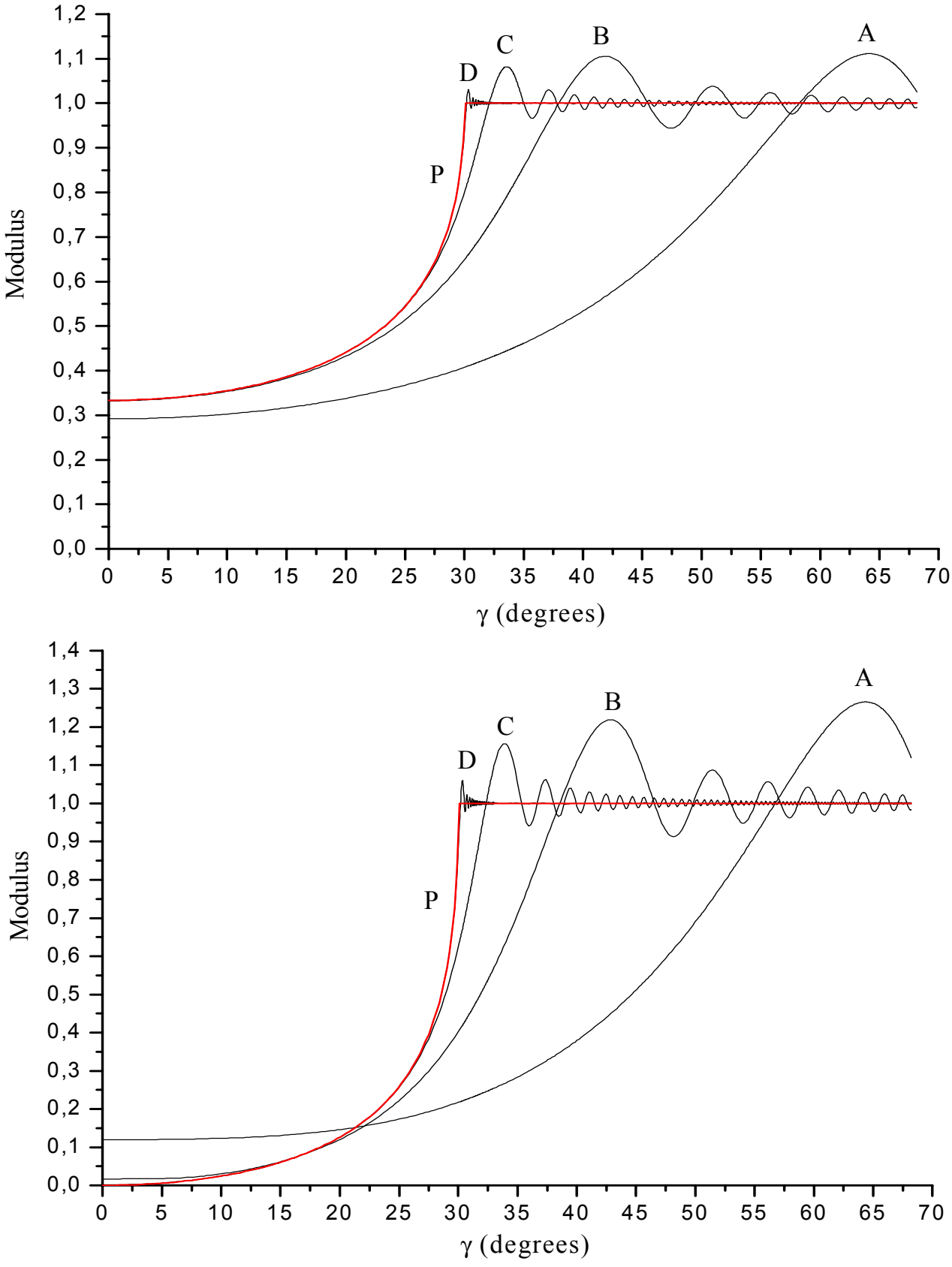


Fig. 1.5. Effective reflection coefficient.

2. TRANSMISSION OPERATOR IN THE TRANSMISSION PROBLEM FOR ELASTIC WAVES

In this Section we discuss analytical properties of the matrix transmission operator for elastic waves, introduce matrices of the effective reflection and transmission coefficients and give their properties. In Subsection 2.1 we give exact statement of the stationary transmission problem for elastic waves. In Subsection 2.2 solution of the problem is represented as sum of given source field and unknown scattered field. In Subsection 2.3 the space scattered field is introduced as result of action of a propagation operator over scattered field trace at the interface. In Subsection 2.4 we derive integral transmission transform at interface. In Subsection 2.5 we derive matrix transmission operator. Analytical properties of the transmission operator are analyzed. Its scalar elements, which are represented by reflection and transmission operators, are introduced through the Fourier transform in the domain of space frequencies and linear combinations of classical elastic plane-wave reflection and transmission coefficients. In Subsection 2.6 action of this operator over the vertical and horizontal components of the source field trace is reduced to the pointwise multiplication with the matrix of corresponding effective coefficients. It is shown that the effective coefficients tend to corresponding plane-wave coefficients when angular frequency tends to infinity. Graphs of vertical and horizontal components of the effective coefficient of monotype reflection for various density contrasts are brought.

2.1. Statement of the canonical problem

Let notations for coordinates and unit normal be the same as is Subsection 1.1 (Fig. 2.1). The propagation of elastic waves in half-space $\Omega_j \subset \mathrm{R}^3$, $j = 1,2$ is usually expressed in terms of the displacement vector $\mathrm{u}_j(\mathrm{x}) = \left(u_{j,1}, u_{j,2}, u_{j,3}\right)$, $\mathrm{x} \in \Omega_j$ and the stress tensor $\mathrm{T}_j\left(\mathrm{u}_j\right) = \left[T_{j,mn}\right]$ [36]. For isotropic elastic solid Ω_j with Lame constants λ_j and μ_j, the stress tensor is connected to the displacement vector by the relation

$$\mathrm{T}_j\left(\mathrm{u}_j\right) = \lambda_j \nabla \cdot \mathrm{u}_j \, \mathrm{I} + \mu_j \left(\nabla \mathrm{u}_j + \mathrm{u}_j \nabla\right) \tag{2.1}$$

and has scalar components

$$T_{j,mn}\left(\mathrm{u}_j\right) = \lambda_j \delta_{mn} \nabla \cdot \mathrm{u}_j + \mu_j \left(\frac{\partial u_{j,m}}{\partial x_n} + \frac{\partial u_{j,n}}{\partial x_m} \right) \tag{2.2}$$

Introduce additional notation for the traction vector

$$\mathrm{t}_j = \mathrm{T}_j\left(\mathrm{u}_j\right)\mathrm{n}_j \tag{2.3}$$

The canonical transmission problem consists in finding pair of the displacement fields $\mathrm{u}_j(\mathrm{x}) \in H^1_{loc}\left(\Omega_j\right)$, which satisfy the stationary equation of wave motion

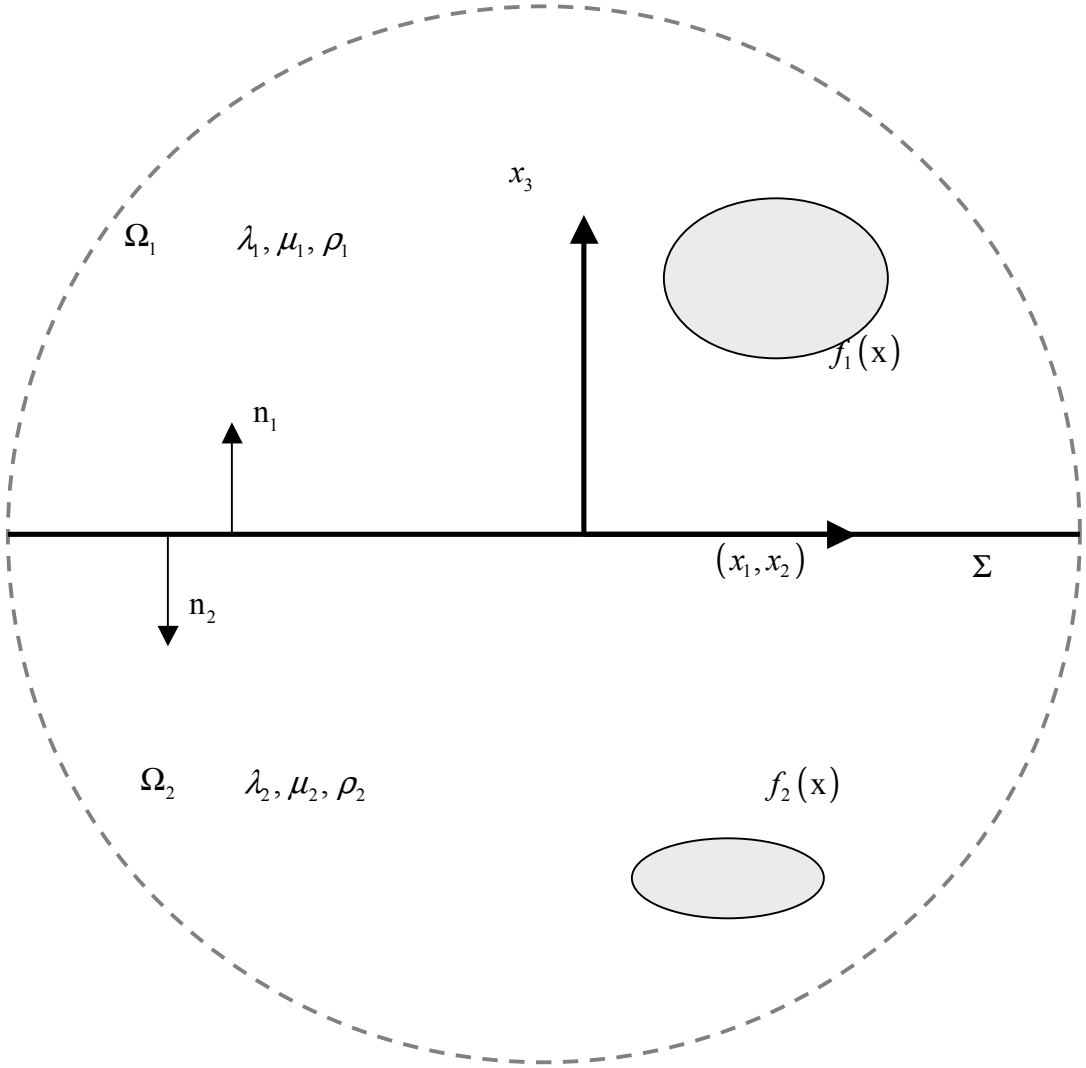


Fig. 2.1. Medium model.

$$\nabla \cdot \mathrm{T}_j\left(\mathrm{u}_j\right)+\rho_j\omega^2\mathrm{u}_j=-\mathrm{f}_j, \tag{2.4}$$

where ρ_j is the medium density and $\mathrm{f}_j(\mathrm{x})$ is vector of the volume density of sources, concluded inside the support $\operatorname{supp}\mathrm{f}_j \subset \Omega_j$. We will consider partial case of the volume density of sources. Introduce ort $\mathrm{e}_\theta=(-\sin\theta,\cos\theta,0)$. Let the density $\mathrm{f}_j(\mathrm{x})$ in equation (2.4) have the form of sum of two directed forces: the first one has normal direction to the interface Σ and generates P and SV waves, the second one generates only SH waves. Then the volume density takes the form

$$\mathrm{f}_j(\mathrm{x})=f_{zj}(\mathrm{x})\mathrm{e}_3+f_{\theta j}(\mathrm{x})\mathrm{e}_\theta \tag{2.5}$$

Additionally we require the displacement field to satisfy radiation conditions when $|\mathrm{x}|\to\infty$ [21]

$$\mathrm{u}_j=o(1),\quad \partial\mathrm{u}_{\alpha j}/\partial|\mathrm{x}|-ik_{\alpha j}\mathrm{u}_{\alpha j}=O\left(|\mathrm{x}|^{-1}\right), \tag{2.6}$$

where the index $\alpha=P,S$ corresponds to longitudinal and shear waves, $k_{\alpha j}=\omega/c_{\alpha j}$ are the wave numbers, $c_{Pj}=\sqrt{(\lambda_j+2\mu_j)/\rho_j}$ and $c_{Sj}=\sqrt{\mu_j/\rho_j}$ are constant P and S wave propagation velocities in Ω_j correspondingly. The complete wave fields satisfy the transmission conditions at interface

$$\mathrm{u}_1=\mathrm{u}_2,\quad \mathrm{t}_1=-\mathrm{t}_2 \tag{2.7}$$

There exist unique solution of the problem (2.4)-(2.7) (see corresponding references in [21]).

2.2. Space source field

Solution of the problem in each half-space may be represented as sum of given source field and unknown scattered field

$$\mathrm{u}_j(\mathrm{x})=\mathrm{u}_j^-(\mathrm{x})+\mathrm{u}_j^+(\mathrm{x}) \tag{2.8}$$

Taking into account representation (2.5), the source field has form of sum of one longitudinal and two shear waves

$$\mathrm{u}_j^-(\mathrm{x})=\mathrm{u}_{Pj}^-(\mathrm{x})+\mathrm{u}_{SVj}^-(\mathrm{x})+\mathrm{u}_{SHj}^-(\mathrm{x}), \tag{2.9}$$

where

$$
\begin{aligned}
\mathrm{u}^{-}_{Pj}(\mathrm{x}) &= \iiint\limits_{\mathrm{supp}\,\mathrm{f}_j} f_{zj}(\mathrm{x}')\mathrm{e}_3\,\mathrm{G}_{Pj}(\mathrm{x},\mathrm{x}')\,d\mathrm{x}', \\
\mathrm{u}^{-}_{SVj}(\mathrm{x}) &= \iiint\limits_{\mathrm{supp}\,\mathrm{f}_j} f_{zj}(\mathrm{x}')\mathrm{e}_3\,\mathrm{G}_{Sj}(\mathrm{x},\mathrm{x}')\,d\mathrm{x}', \\
\mathrm{u}^{-}_{SHj}(\mathrm{x}) &= \iiint\limits_{\mathrm{supp}\,\mathrm{f}_j} f_{\theta j}(\mathrm{x}')\mathrm{e}_\theta\,\mathrm{G}_{Sj}(\mathrm{x},\mathrm{x}')\,d\mathrm{x}'
\end{aligned}
\tag{2.10}
$$

In (2.10) we introduced the fundamental tensor $\mathrm{G}_j(\mathrm{x},\mathrm{x}') = \left[G_{j,mn}\right]$ as two-point function of space coordinates

$$
\mathrm{G}_j(\mathrm{x},\mathrm{x}') = \frac{1}{\rho_j\omega^2}\left[k_{Sj}^2\, g_{Sj}(\mathrm{x},\mathrm{x}')\mathrm{I} - \nabla\left[g_{Pj}(\mathrm{x},\mathrm{x}') - g_{Sj}(\mathrm{x},\mathrm{x}')\right]\nabla\right] \tag{2.11}
$$

In component-wise notations, the tensor (2.11) has form

$$
G_{j,mn}(\mathrm{x},\mathrm{x}') = \frac{1}{\rho_j\omega^2}\left[k_{Sj}^2\, g_{Sj}(\mathrm{x},\mathrm{x}')\delta_{mn} - \frac{\partial}{\partial x_m}\frac{\partial}{\partial x_n}\left[g_{Pj}(\mathrm{x},\mathrm{x}') - g_{Sj}(\mathrm{x},\mathrm{x}')\right]\right] \tag{2.12}
$$

Components of the fundamental tensor may be expressed through the scalar fundamental solutions defined by formulas $g_{\alpha j}(\mathrm{x},\mathrm{x}') = \exp\left(ik_{\alpha j}\left|\mathrm{x}-\mathrm{x}'\right|\right)\Big/4\pi\left|\mathrm{x}-\mathrm{x}'\right|$, as in Subsection 1.2.

Introduce notation for the Weyl transform

$$
\hat{E}^{\pm}_{\alpha j}(x_3) = \exp\left(\pm i\varepsilon_j\zeta_{\alpha j}x_3\right), \quad \zeta_{\alpha j} = \sqrt{k_{\alpha j}^2 - \left(\zeta_1^2+\zeta_2^2\right)} \tag{2.13}
$$

and introduce representation for the scalar fundamental solutions $g_{\alpha j}(\mathrm{x},\mathrm{x}')$ over the complete system of elastic plane waves, outgoing from Σ into half-space $\mathrm{R}^3\big/\overline{\Omega}_j$,

$$
g_{\alpha j}(\mathrm{x},\mathrm{x}') = F\left[\hat{g}_{\alpha j}(\overline{\mathrm{x}}')\hat{E}^{-}_{\alpha j}(x_3 - x_3')\right] \tag{2.14}
$$

In (2.14) spectra of the fundamental solutions are given by the formulas $\hat{g}_{\alpha j}(\overline{\mathrm{x}}') = i\exp\left[-i\left(\zeta_1 x_1' + \zeta_2 x_2'\right)\right]\Big/4\pi\zeta_{\alpha j}$.

Introduce also notation for the wave vectors of longitudinal and shear waves

$$
\mathrm{k}^{\pm}_{\alpha j} = \left(\zeta_1, \zeta_2, \pm\varepsilon_j\zeta_{\alpha j}\right) \tag{2.15}
$$

In these assumptions, the fundamental tensor (2.11) may be rewritten as sum of two tensors, which correspond to longitudinal and shear waves,

$$
\mathrm{G}_j(\mathrm{x},\mathrm{x}') = \mathrm{G}_{Pj}(\mathrm{x},\mathrm{x}') + \mathrm{G}_{Sj}(\mathrm{x},\mathrm{x}'), \tag{2.16}
$$

where

$$\mathrm{G}_{Pj}\left(\mathrm{x},\mathrm{x}'\right)=F\left[\frac{\hat{g}_{Pj}\left(\bar{\mathrm{x}}'\right)}{\rho_j\omega^2}\left(\mathrm{k}_{Pj}^{-}\otimes\mathrm{k}_{Pj}^{-}\right)\hat{E}_{Pj}^{-}\left(x_3-x_3'\right)\right],$$
$$\mathrm{G}_{Sj}\left(\mathrm{x},\mathrm{x}'\right)=F\left[\frac{\hat{g}_{Sj}\left(\bar{\mathrm{x}}'\right)}{\rho_j\omega^2}\left(k_{Sj}^2\mathrm{I}-\mathrm{k}_{Sj}^{-}\otimes\mathrm{k}_{Sj}^{-}\right)\hat{E}_{Sj}^{-}\left(x_3-x_3'\right)\right], \tag{2.17}$$

dyads $\mathrm{k}_{\alpha j}^{-}\otimes\mathrm{k}_{\alpha j}^{-}$ are given by the formulas

$$\mathrm{k}_{\alpha j}^{-}\otimes\mathrm{k}_{\alpha j}^{-}=\begin{bmatrix}\zeta_1^2 & \zeta_1\zeta_2 & -\varepsilon_j\zeta_1\zeta_{\alpha j}\\ \zeta_1\zeta_2 & \zeta_2^2 & -\varepsilon_j\zeta_2\zeta_{\alpha j}\\ -\varepsilon_j\zeta_1\zeta_{\alpha j} & -\varepsilon_j\zeta_2\zeta_{\alpha j} & \zeta_{\alpha j}^2\end{bmatrix} \tag{2.18}$$

Substitution of (2.17) into relations (2.10) gives spectral representations for all the components of the source field in the form

$$\mathrm{u}_{\alpha j}^{-}\left(\mathrm{x}\right)=F\left[\hat{a}_{\alpha j}^{-}\,\mathrm{p}_{\alpha j}^{-}\,\hat{E}_{\alpha j}^{-}\left(x_3\right)\right],\quad \alpha=P,SV,SH\,, \tag{2.19}$$

where $\hat{E}_{SVj}^{-}\left(x_3\right)=\hat{E}_{SHj}^{-}\left(x_3\right)=\hat{E}_{Sj}^{-}\left(x_3\right)$, $\mathrm{p}_{\alpha j}^{-}$ are polarization vectors of incident P, SV and SH waves. Taking into account normalization condition for the angular component $\mathrm{u}_{SHj}^{-}\left(\mathrm{x}\right)$ from (2.10) [13], the spectral amplitudes $\hat{a}_{\alpha j}^{-}$ are

$$\hat{a}_{Pj}^{-}=\frac{-\varepsilon_j\zeta_{Pj}k_{Pj}}{\rho_j\omega^2}\iiint\limits_{\mathrm{supp}\,\mathrm{f}_j}f_{zj}\left(\mathrm{x}'\right)\hat{g}_{Pj}\left(\bar{\mathrm{x}}'\right)\hat{E}_{Pj}^{-}\left(-x_3'\right)d\mathrm{x}',$$
$$\hat{a}_{SVj}^{-}=\frac{\varepsilon_j\zeta\,k_{Sj}}{\rho_j\omega^2}\iiint\limits_{\mathrm{supp}\,\mathrm{f}_j}f_{zj}\left(\mathrm{x}'\right)\hat{g}_{Sj}\left(\bar{\mathrm{x}}'\right)\hat{E}_{Sj}^{-}\left(-x_3'\right)d\mathrm{x}', \tag{2.20}$$
$$\hat{a}_{SHj}^{-}=\frac{\varepsilon_j\zeta^2\cos\left(\varphi-\theta\right)}{\rho_j\omega^2}\iiint\limits_{\mathrm{supp}\,\mathrm{f}_j}f_{\theta j}\left(\mathrm{x}'\right)\hat{g}_{Sj}\left(\bar{\mathrm{x}}'\right)\hat{E}_{Sj}^{-}\left(-x_3'\right)d\mathrm{x}'$$

In polar coordinates $\zeta_1=\zeta\cos\varphi,\ \zeta_2=\zeta\sin\varphi$ at the plane of space frequencies $\left(\zeta_1,\zeta_2\right)$, the polarization vectors for incident and scattered P, SV and SH waves may be introduced as

$$\mathrm{p}_{Pj}^{\pm}=\frac{1}{k_{Pj}}\mathrm{k}_{Pj}^{\pm}=\frac{1}{k_{Pj}}\left(\zeta\cos\varphi,\zeta\sin\varphi,\pm\varepsilon_j\zeta_{Pj}\right),$$
$$\mathrm{p}_{SVj}^{\pm}=\mp\frac{1}{k_{Sj}\zeta}\left(\mathrm{k}_{Sj}^{\pm}\times\varepsilon_j\mathrm{e}_3\right)\times\mathrm{k}_{Sj}^{\pm}=\frac{1}{k_{Sj}}\left(\zeta_{Sj}\cos\varphi,\zeta_{Sj}\sin\varphi,\mp\varepsilon_j\zeta\right), \tag{2.21}$$
$$\mathrm{p}_{SHj}^{\pm}=\mp\frac{1}{k_{Sj}}\mathrm{k}_{Sj}^{\pm}\times\mathrm{p}_{SVj}^{\pm}=\varepsilon_j\left(\sin\varphi,-\cos\varphi,0\right)$$

2.3. Space scattered field

Let us seek an unknown scattered field in the form of sum of one longitudinal and two shear waves

$$\mathrm{u}_j^+(\mathrm{x}) = \mathrm{u}_{Pj}^+(\mathrm{x}) + \mathrm{u}_{SVj}^+(\mathrm{x}) + \mathrm{u}_{SHj}^+(\mathrm{x}) \tag{2.22}$$

By analogy with the representation of the source field through the waves incoming to the interface, it is reasonable that we represent the scattered field in the form of the Weyl transform over the complete system of the elastic plane waves outgoing from the interface Σ into half-space Ω_j, i.e.

$$\mathrm{u}_{\alpha j}^+(\mathrm{x}) = F\left[\hat{a}_{\alpha j}^+ \; \mathrm{p}_{\alpha j}^+ \; \hat{E}_{\alpha j}^+(x_3)\right] \tag{2.23}$$

Let us obtain the desired representation of the space scattered wave field as action of the propagation operator on its trace at the interface. For this aim, we compose six-dimensional vectors of the source fields and scattered fields is each half-space, which contain Cartesian coordinates: $\mathbf{u}^{\pm}(\mathrm{x}) = \left(\mathrm{u}_1^{\pm}, \mathrm{u}_2^{\pm}\right)$ and corresponding spectral vectors $\hat{\mathbf{u}}^{\pm} = \left(\hat{\mathrm{u}}_1^{\pm}, \hat{\mathrm{u}}_2^{\pm}\right)$, $\hat{\mathrm{u}}_j^{\pm} = \left(\hat{u}_{Pj}^{\pm}, \hat{u}_{SVj}^{\pm}, \hat{u}_{SHj}^{\pm}\right)$. Introduce also six-dimensional vectors of spectral amplitudes of P, SV and SH waves $\hat{\mathbf{a}}^{\pm} = \left(\hat{\mathrm{a}}_1^{\pm}, \hat{\mathrm{a}}_2^{\pm}\right)$, $\hat{\mathrm{a}}_j^{\pm} = \left(\hat{a}_{Pj}^{\pm}, \hat{a}_{SVj}^{\pm}, \hat{a}_{SHj}^{\pm}\right)$, which are connected with the vectors $\hat{\mathbf{u}}^{\pm}$ by the formula

$$\hat{\mathbf{u}}^{\pm} = \hat{\mathbf{A}}^{\pm}\hat{\mathbf{a}}^{\pm}, \tag{2.24}$$

where

$$\hat{\mathbf{A}}^{\pm} = diag\left\{\hat{\mathrm{A}}_1^{\pm}, \hat{\mathrm{A}}_2^{\pm}\right\}, \tag{2.25}$$

$$\hat{\mathrm{A}}_j^{\pm} = \left[\hat{A}_{j,m\alpha}^{\pm}\right] = \left[\left(\mathrm{e}_m, \mathrm{p}_{\alpha j}^{\pm}\right)\right] = \begin{bmatrix} \zeta_1/k_{Pj} & \zeta_{Sj}\zeta_1/\left(k_{Sj}\zeta\right) & \varepsilon_j\,\zeta_2/\zeta \\ \zeta_2/k_{Pj} & \zeta_{Sj}\zeta_2/\left(k_{Sj}\zeta\right) & -\varepsilon_j\,\zeta_1/\zeta \\ \pm\varepsilon_j\zeta_{Pj}/k_{Pj} & \mp\varepsilon_j\zeta/k_{Sj} & 0 \end{bmatrix} \tag{2.26}$$

Introduce six-dimensional matrix consisting of the Weyl transforms for scattered waves: $\hat{\mathbf{E}}^+(x_3) = diag\left\{\hat{\mathrm{E}}_1^+, \hat{\mathrm{E}}_2^+\right\}$, $\hat{\mathrm{E}}_j^+(x_3) = diag\left\{\hat{\mathrm{E}}_{Pj}^+, \hat{\mathrm{E}}_{Sj}^+, \hat{\mathrm{E}}_{Sj}^+\right\}$. In such notations, from formulas (2.22) -(2.24) it follows that

$$\mathbf{u}^+(\mathrm{x}) = F\,\hat{\mathbf{A}}^+\hat{\mathbf{E}}^+\left(\hat{\mathbf{A}}^+\right)^{-1}\hat{\mathbf{u}}^+ \tag{2.27}$$

From the relation (2.27) when $x_3 \to 0$ it trivially follows that $\mathbf{u}^+\left(\overline{\mathrm{x}}_j\right) = F\,\hat{\mathbf{u}}^+$. Evaluating the spectral vector $\hat{\mathbf{u}}^+$ and substituting it to (2.27), we obtain

$$\mathbf{u}^{+}\left(\mathrm{x}\right)=\mathbf{P}^{+}\mathbf{u}^{+}\left(\overline{\mathrm{x}}_{j}\right), \tag{2.28}$$

where the operator

$$\mathbf{P}^{+}=F\,\hat{\mathbf{A}}^{+}\hat{\mathbf{E}}^{+}\left(\hat{\mathbf{A}}^{+}\right)^{-1}F^{-1} \tag{2.29}$$

is a propagation operator, which allows to regenerate unknown scattered field $\mathbf{u}^{+}\left(\mathrm{x}\right)$ using its trace $\mathbf{u}^{+}\left(\overline{\mathrm{x}}_{j}\right)$ at the interface. Notice that, as in acoustic case, this trace is an unknown function.

2.4. Transmission transform at interface of half-spaces

Express the unknown trace $\mathbf{u}^{+}\left(\overline{\mathrm{x}}_{j}\right)$ through the given trace $\mathbf{u}^{-}\left(\overline{\mathrm{x}}_{j}\right)$ with help of the transmission transform. Since the Lame equation (2.4) and conditions (2.6) are taken into consideration for derivation of the relation (2.28), to derive the transmission transform it is necessary to turn to the transmission conditions (2.7). Substituting solution (2.8) in the transmission conditions (2.7) and applying the inverse Fourier transform to both parts of the transmission conditions, we obtain spectral form of the transmission conditions

$$\hat{\mathrm{u}}_{1}^{+}+\hat{\mathrm{u}}_{1}^{-}=\hat{\mathrm{u}}_{2}^{+}+\hat{\mathrm{u}}_{2}^{-},\quad \hat{\mathrm{t}}_{1}^{+}+\hat{\mathrm{t}}_{1}^{-}=-\left(\hat{\mathrm{t}}_{2}^{+}+\hat{\mathrm{t}}_{2}^{-}\right) \tag{2.30}$$

To reduce spectral conditions (2.30) to a system of equations for $\hat{\mathrm{u}}_{j}^{+}$, let us consider the dependence between vectors $\hat{\mathrm{u}}_{j}^{\pm}$ and corresponding spectral analogue of the traction vectors $\hat{\mathrm{t}}_{j}^{\pm}=\left(\hat{t}_{j,1}^{\pm},\hat{t}_{j,2}^{\pm},\hat{t}_{j,3}^{\pm}\right)$ in Cartesian coordinates. Substitution of the Fourier representations for the components from (2.9) and (2.22) in the definition of the traction vector (2.3) gives the desired interconnection in the form

$$\hat{\mathrm{t}}_{j}^{\pm}=\hat{\mathrm{Q}}_{j}^{\pm}\,\hat{\mathrm{u}}_{j}^{\pm}, \tag{2.31}$$

where the matrices

$$\hat{\mathrm{Q}}_{j}^{\pm}=\begin{bmatrix} -\dfrac{i\varepsilon_{j}\mu_{j}\zeta\left(-2\zeta_{Pj}\zeta_{Sj}+\zeta_{Sj}^{2}-\zeta^{2}\right)}{\zeta^{2}+\zeta_{Pj}\zeta_{Sj}} & \pm\dfrac{i\mu_{j}\zeta_{Pj}k_{Sj}^{2}}{\cos\left(\varphi-\theta\right)\left(\zeta^{2}+\zeta_{Pj}\zeta_{Sj}\right)} & 0 \\ \pm\dfrac{i\left(\lambda_{j}k_{Pj}^{2}\zeta_{Sj}+2\mu_{j}\zeta_{Pj}^{2}\zeta_{Sj}+2\mu_{j}\zeta^{3}\right)}{\zeta^{2}+\zeta_{Pj}\zeta_{Sj}} & -\dfrac{i\varepsilon_{j}\zeta\left(-\lambda_{j}k_{Pj}^{2}-2\mu_{j}\zeta_{Pj}^{2}+2\mu_{j}\zeta\zeta_{Pj}\right)}{\cos\left(\varphi-\theta\right)\left(\zeta^{2}+\zeta_{Pj}\zeta_{Sj}\right)} & 0 \\ 0 & 0 & \pm i\mu_{j}\zeta_{Sj} \end{bmatrix} \tag{2.32}$$

are spectral analogues of the operator $\mathrm{T}_j(\cdot)\mathrm{n}_j$.

Substitute (2.31) in (2.30) and move the unknown spectra $\hat{\mathrm{u}}_j^+$ to the left-hand part of the system (2.30), and the given spectra $\hat{\mathrm{u}}_j^-$ to its right-hand part. Then the system takes matrix form

$$\hat{\mathbf{L}}^+\hat{\mathbf{u}}^+ = \hat{\mathbf{L}}^-\hat{\mathbf{u}}^-, \tag{2.33}$$

where

$$\hat{\mathbf{L}}^\pm = \begin{bmatrix} \pm\mathrm{I} & \mp\mathrm{I} \\ \pm\hat{\mathrm{Q}}_1^\pm & \mp\hat{\mathrm{Q}}_2^\pm \end{bmatrix} \tag{2.34}$$

Owing to the fact that determinant of the matrix $\hat{\mathbf{L}}^+$ is not equal to zero, we multiply the equality (2.33) by $\left(\hat{\mathbf{L}}^+\right)^{-1}$ from the left. Then we obtain desired dependence between vectors $\hat{\mathbf{u}}^+$ and $\hat{\mathbf{u}}^-$ in the form

$$\hat{\mathbf{u}}^+ = \hat{\mathbf{T}}_D\,\hat{\mathbf{u}}^-, \tag{2.35}$$

where

$$\hat{\mathbf{T}}_D = \left(\hat{\mathbf{L}}^+\right)^{-1}\hat{\mathbf{L}}^- = \begin{bmatrix} \left(\mathrm{I}-\left(\hat{\mathrm{Q}}_2^+\right)^{-1}\hat{\mathrm{Q}}_1^+\right)^{-1} & \left(\hat{\mathrm{Q}}_1^+-\hat{\mathrm{Q}}_2^+\right)^{-1} \\ \left(\left(\hat{\mathrm{Q}}_1^+\right)^{-1}\hat{\mathrm{Q}}_2^+-\mathrm{I}\right)^{-1} & \left(\hat{\mathrm{Q}}_1^+-\hat{\mathrm{Q}}_2^+\right)^{-1} \end{bmatrix} \tag{2.36}$$

Substituting the Fourier transform $\hat{\mathbf{u}}^- = F^{-1}\mathbf{u}^-\left(\overline{\mathrm{y}}_j\right)$ and $\hat{\mathbf{u}}^+ = F^{-1}\mathbf{u}^+\left(\overline{\mathrm{x}}_j\right)$ in the relation (2.35), we obtain the desired transmission transform at the interface in the form

$$\mathbf{u}^+\left(\overline{\mathrm{x}}_j\right) = F\,\hat{\mathbf{T}}_D\,F^{-1}\,\mathbf{u}^-\left(\overline{\mathrm{y}}_j\right) \tag{2.37}$$

2.5. Transmission operator

Let us show that the scalar elements of the spectral matrix (2.36) may be expressed through the classical coefficients of elastic plane waves. For that substitute corresponding relations from (2.24) in the left-hand and right-hand parts of (2.35). As a result we obtain

$$\hat{\mathbf{a}}^+ = \hat{\mathbf{K}}\,\hat{\mathbf{a}}^-, \tag{2.38}$$

where

$$\hat{\mathbf{K}} = \left(\hat{\mathbf{A}}^{+}\right)^{-1} \hat{\mathbf{T}}_D \hat{\mathbf{A}}^{-} = \begin{bmatrix} \hat{\mathrm{K}}^{11} & \hat{\mathrm{K}}^{12} \\ \hat{\mathrm{K}}^{21} & \hat{\mathrm{K}}^{22} \end{bmatrix}, \tag{2.39}$$

$$\hat{\mathrm{K}}^{mn} = \begin{bmatrix} \hat{k}_{PP}^{mn} & \hat{k}_{PSV}^{mn} & 0 \\ \hat{k}_{SVP}^{mn} & \hat{k}_{SVSV}^{mn} & 0 \\ 0 & 0 & \hat{k}_{SHSH}^{mn} \end{bmatrix}, \tag{2.40}$$

$$\hat{k}_{PP}^{11} = \frac{\left(bw_{P1} - cw_{P2}\right)\left(bw_{S1} + cw_{S2}\right) - \eta^2\left(a + dw_{P1}w_{S2}\right)\left(a - dw_{P2}w_{S1}\right)}{\left(bw_{P1} + cw_{P2}\right)\left(bw_{S1} + cw_{S2}\right) + \eta^2\left(a - dw_{P1}w_{S2}\right)\left(a - dw_{P2}w_{S1}\right)},$$

$$\hat{k}_{SVP}^{11} = -2\frac{c_{P1}}{c_{S1}} w_{S1} \frac{\eta\left(ab + cdw_{P2}w_{S2}\right)}{\left(bw_{P1} + cw_{P2}\right)\left(bw_{S1} + cw_{S2}\right) + \eta^2\left(a - dw_{P1}w_{S2}\right)\left(a - dw_{P2}w_{S1}\right)},$$

$$\hat{k}_{PSV}^{11} = -2\frac{c_{S1}}{c_{P1}} w_{S1} \frac{\eta\left(ab + cdw_{P2}w_{S2}\right)}{\left(bw_{P1} + cw_{P2}\right)\left(bw_{S1} + cw_{S2}\right) + \eta^2\left(a - dw_{P1}w_{S2}\right)\left(a - dw_{P2}w_{S1}\right)},$$

$$\hat{k}_{SVSV}^{11} = -\frac{\left(bw_{P1} + cw_{P2}\right)\left(bw_{S1} - cw_{S2}\right) - \eta^2\left(a - dw_{P1}w_{S2}\right)\left(a + dw_{P2}w_{S1}\right)}{\left(bw_{P1} + cw_{P2}\right)\left(bw_{S1} + cw_{S2}\right) + \eta^2\left(a - dw_{P1}w_{S2}\right)\left(a - dw_{P2}w_{S1}\right)},$$

$$\hat{k}_{SHSH}^{11} = \frac{\mu_1\zeta_{S1} - \mu_2\zeta_{S2}}{\mu_1\zeta_{S1} + \mu_2\zeta_{S2}},$$

$$\hat{k}_{PP}^{12} = 2\rho_2 \frac{c_{P2}}{c_{P1}} w_{P2} \frac{bw_{S1} + cw_{S2}}{\left(bw_{P1} + cw_{P2}\right)\left(bw_{S1} + cw_{S2}\right) + \eta^2\left(a - dw_{P1}w_{S2}\right)\left(a - dw_{P2}w_{S1}\right)},$$

$$\hat{k}_{SVP}^{12} = -2\rho_2 \frac{c_{P2}}{c_{S1}} w_{P2} \frac{\eta\left(a - dw_{P1}w_{S2}\right)}{\left(bw_{P1} + cw_{P2}\right)\left(bw_{S1} + cw_{S2}\right) + \eta^2\left(a - dw_{P1}w_{S2}\right)\left(a - dw_{P2}w_{S1}\right)},$$

$$\hat{k}_{PSV}^{12} = 2\rho_2 \frac{c_{S2}}{c_{P1}} w_{P2} \frac{\eta\left(a - dw_{P2}w_{S1}\right)}{\left(bw_{P1} + cw_{P2}\right)\left(bw_{S1} + cw_{S2}\right) + \eta^2\left(a - dw_{P1}w_{S2}\right)\left(a - dw_{P2}w_{S1}\right)},$$

$$\hat{k}_{SVSV}^{12} = 2\rho_2 \frac{c_{S2}}{c_{S1}} w_{S2} \frac{bw_{P1} + cw_{P2}}{\left(bw_{P1} + cw_{P2}\right)\left(bw_{S1} + cw_{S2}\right) + \eta^2\left(a - dw_{P1}w_{S2}\right)\left(a - dw_{P2}w_{S1}\right)},$$

$$\hat{k}_{SHSH}^{12} = 1 - \hat{k}_{SHSH}^{11},$$

$$\hat{k}_{PP}^{21} = 2\rho_1 \frac{c_{P1}}{c_{P2}} w_{P1} \frac{bw_{S1} + cw_{S2}}{\left(bw_{P1} + cw_{P2}\right)\left(bw_{S1} + cw_{S2}\right) + \eta^2\left(a - dw_{P1}w_{S2}\right)\left(a - dw_{P2}w_{S1}\right)},$$

$$\hat{k}_{SVP}^{21} = 2\rho_1 \frac{c_{P1}}{c_{S2}} w_{P1} \frac{\eta\left(a - dw_{P2}w_{S1}\right)}{\left(bw_{P1} + cw_{P2}\right)\left(bw_{S1} + cw_{S2}\right) + \eta^2\left(a - dw_{P1}w_{S2}\right)\left(a - dw_{P2}w_{S1}\right)},$$

$$\hat{k}_{PSV}^{21} = -2\rho_1 \frac{c_{S1}}{c_{P2}} w_{S1} \frac{\eta\left(a - dw_{P1}w_{S2}\right)}{\left(bw_{P1} + cw_{P2}\right)\left(bw_{S1} + cw_{S2}\right) + \eta^2\left(a - dw_{P1}w_{S2}\right)\left(a - dw_{P2}w_{S1}\right)}, \tag{2.41}$$

$$\hat{k}_{SVSV}^{21} = 2\rho_1 \frac{c_{S1}}{c_{S2}} w_{S1} \frac{bw_{P1} + cw_{P2}}{\left(bw_{P1} + cw_{P2}\right)\left(bw_{S1} + cw_{S2}\right) + \eta^2\left(a - dw_{P1}w_{S2}\right)\left(a - dw_{P2}w_{S1}\right)},$$

$$\hat{k}_{SHSH}^{21} = 1 + \hat{k}_{SHSH}^{11},$$

$$\hat{k}_{PP}^{22}=-\frac{(bw_{P1}-cw_{P2})(bw_{S1}+cw_{S2})+\eta^2(a-dw_{P1}w_{S2})(a+dw_{P2}w_{S1})}{(bw_{P1}+cw_{P2})(bw_{S1}+cw_{S2})+\eta^2(a-dw_{P1}w_{S2})(a-dw_{P2}w_{S1})},$$

$$\hat{k}_{SVP}^{22}=2\frac{c_{P2}}{c_{S2}}w_{P2}\frac{\eta(ac+bdw_{P1}w_{S1})}{(bw_{P1}+cw_{P2})(bw_{S1}+cw_{S2})+\eta^2(a-dw_{P1}w_{S2})(a-dw_{P2}w_{S1})},$$

$$\hat{k}_{PSV}^{22}=2\frac{c_{S2}}{c_{P2}}w_{S2}\frac{\eta(ac+bdw_{P1}w_{S1})}{(bw_{P1}+cw_{P2})(bw_{S1}+cw_{S2})+\eta^2(a-dw_{P1}w_{S2})(a-dw_{P2}w_{S1})},$$

$$\hat{k}_{SVSV}^{22}=\frac{(bw_{P1}+cw_{P2})(bw_{S1}-cw_{S2})+\eta^2(a+dw_{P1}w_{S2})(a-dw_{P2}w_{S1})}{(bw_{P1}+cw_{P2})(bw_{S1}+cw_{S2})+\eta^2(a-dw_{P1}w_{S2})(a-dw_{P2}w_{S1})},$$

$$\hat{k}_{SHSH}^{22}=-\hat{k}_{SHSH}^{11}$$

In the formulas (2.41) we introduced notation $\eta=\zeta/\omega$, parameters

$$d=2\left(\rho_2c_{S2}^2-\rho_1c_{S1}^2\right),\quad a(\eta)=\rho_2-\rho_1-d\eta^2,$$
$$b(\eta)=\rho_2-d\eta^2,\quad c(\eta)=\rho_1+d\eta^2 \tag{2.42}$$

and expressions

$$w_{P1}=\zeta_{P1}/\omega=\sqrt{c_{P1}^{-2}-\eta^2},\quad w_{S1}=\zeta_{S1}/\omega=\sqrt{c_{S1}^{-2}-\eta^2},$$
$$w_{P2}=\zeta_{P2}/\omega=\sqrt{c_{P2}^{-2}-\eta^2},\quad w_{S2}=\zeta_{S2}/\omega=\sqrt{c_{S2}^{-2}-\eta^2} \tag{2.43}$$

Coefficients $\hat{k}_{\alpha\beta}^{mn}$ from (2.41) coincide with the classical elastic reflection and transmission plane-wave coefficients [13, 16, 19]. Symmetry relations for elastic coefficients $\hat{k}_{\alpha\beta}^{mn}$ are brought in [30]. The superscript $mn\,(m,n=1,2)$ corresponds to reflection inside of the medium Ω_n when $m=n$, and transmission from the medium Ω_n into the medium Ω_m when $m\neq n$. The subscript $\alpha\beta\,(\alpha,\beta=P,SV,SH)$ corresponds to conversion of the wave of type β to the wave of type α. Therefore it is natural to term matrices $\hat{\mathrm{K}}^{mn}$ as the reflection matrices when $m=n$ and transmission matrices when $m\neq n$. Notice that the reflection and transmission matrices $\hat{\mathrm{K}}^{mn}$ have block-diagonal structure, which shows that P and SV waves participate in the reflection/transmission process independently on SH waves.

Draw attention on the fact that the matrix $\hat{\mathbf{K}}$ has the property $\hat{\mathbf{K}}^2=\mathbf{I}$. Therefore, by analogy with the acoustic case, from (2.38) it follows that $\left(\hat{\mathbf{a}}^-+\hat{\mathbf{a}}^+\right)=\hat{\mathbf{K}}\left(\hat{\mathbf{a}}^-+\hat{\mathbf{a}}^+\right)$. The vector $\hat{\mathbf{a}}^-+\hat{\mathbf{a}}^+$ is an eigenvector of the matrix $\hat{\mathbf{K}}$ for the eigenvalue $\lambda=1$. However, in contrast to the acoustic case, this property does not have any physical interpretation since the vector $\hat{\mathbf{a}}^-+\hat{\mathbf{a}}^+$ contains only amplitudes of P, SV and SH waves and does not take into consideration polarization vectors.

The matrix $\hat{\mathbf{T}}_D$ does not have block-diagonal form similar to $\hat{\mathbf{K}}$. Therefore we impart it such structure with help of switching to cylindrical coordinates (z, r, θ) in R^3, which are defined by the formulas

$$z = x_3, \quad r = \sqrt{x_1^2 + x_2^2}, \quad \mathrm{tg}\theta = x_2 / x_1 \tag{2.44}$$

Denote vectors of traces of the displacement fields in cylindrical coordinates as $\mathbf{v}^{\pm}(\overline{\mathrm{x}}_j) = (\mathrm{v}_1^{\pm}, \mathrm{v}_2^{\pm})$, $\mathrm{v}_j^{\pm}(\overline{\mathrm{x}}_j) = (v_{j,z}^{\pm}, v_{j,r}^{\pm}, v_{j,\theta}^{\pm})$. Corresponding spectral vectors in cylindrical coordinates have the form $\hat{\mathbf{v}}^{\pm} = (\hat{\mathrm{v}}_1^{\pm}, \hat{\mathrm{v}}_2^{\pm})$, $\hat{\mathrm{v}}_j^{\pm} = (\hat{v}_{j,z}^{\pm}, \hat{v}_{j,r}^{\pm}, \hat{v}_{j,\theta}^{\pm})$. It is evident that each component $\hat{v}_{j,z}^{\pm}$, $\hat{v}_{j,r}^{\pm}$ or $\hat{v}_{j,\theta}^{\pm}$ may be obtained from the scalar product of vector $\hat{\mathrm{u}}_j^{\pm}$ and orts $\mathrm{e}_z = (0,0,1)$, $\mathrm{e}_r = (\cos\theta, \sin\theta, 0)$ or $\mathrm{e}_\theta = (-\sin\theta, \cos\theta, 0)$ of the cylindrical coordinate system. Thus, the connection between vectors $\hat{\mathbf{u}}^{\pm}$ and $\hat{\mathbf{v}}^{\pm}$ has form

$$\hat{\mathbf{v}}^{\pm} = \mathbf{C}\,\hat{\mathbf{u}}^{\pm}, \tag{2.45}$$

where

$$\mathbf{C} = \begin{bmatrix} \mathrm{C} & 0 \\ 0 & \mathrm{C} \end{bmatrix}, \quad \mathrm{C} = \left[C_{qm}\right] = \left[\left(\mathrm{e}_q, \mathrm{e}_m\right)\right] = \begin{bmatrix} 0 & 0 & 1 \\ \cos\theta & \sin\theta & 0 \\ -\sin\theta & \cos\theta & 0 \end{bmatrix}, \quad q = z, r, \theta \tag{2.46}$$

Notice that the dependence between vectors $\mathbf{u}^{\pm}$ and $\mathbf{v}^{\pm}$ is

$$\mathbf{v}^{\pm} = \mathbf{C}\,\mathbf{u}^{\pm} \tag{2.47}$$

Substitution of (2.45) in spectral formula (2.35) gives

$$\hat{\mathbf{v}}^{+} = \hat{\mathbf{T}}\,\hat{\mathbf{v}}^{-}, \tag{2.48}$$

where

$$\hat{\mathbf{T}} = \mathbf{C}\,\hat{\mathbf{T}}_D\,\mathbf{C}^{-1} = \left(\mathbf{C}\hat{\mathbf{A}}^{+}\right)\hat{\mathbf{K}}\left(\mathbf{C}\hat{\mathbf{A}}^{-}\right)^{-1} = \begin{bmatrix} \hat{\mathrm{T}}^{11} & \hat{\mathrm{T}}^{12} \\ \hat{\mathrm{T}}^{21} & \hat{\mathrm{T}}^{22} \end{bmatrix}, \tag{2.49}$$

$$\hat{\mathrm{T}}^{mn} = \begin{bmatrix} \hat{t}_{zz}^{mn} & \hat{t}_{zr}^{mn} & 0 \\ \hat{t}_{rz}^{mn} & \hat{t}_{rr}^{mn} & 0 \\ 0 & 0 & \hat{t}_{\theta\theta}^{mn} \end{bmatrix} \tag{2.50}$$

The superscript $mn\,(m, n = 1, 2)$ corresponds to reflection inside of the medium Ω_n when $m = n$, and transmission from the medium Ω_n into the medium Ω_m when $m \neq n$. The

subscript $pq\,(p,q=z,r,\theta)$ corresponds to conversion of the component with index q to the component with index p. The structure of $\hat{\mathrm{T}}^{mn}$ in (2.50) shows that in the reflection/transmission process vertical and radial components of the displacement fields are connected and do not mix with angular components of these fields. Physically it means that P and SV waves interfere during transmission at the interface independently on SH waves.

Substituting Fourier transform in relation (2.48), we obtain the transmission transform in the cylindrical coordinates

$$\mathbf{v}^{+}\left(\overline{\mathrm{x}}_{j}\right)=\mathbf{T}\,\mathbf{v}^{-}\left(\overline{\mathrm{y}}_{j}\right), \tag{2.51}$$

where

$$\mathbf{T}=F\,\hat{\mathbf{T}}\,F^{-1}=\begin{bmatrix}\mathrm{T}^{11} & \mathrm{T}^{12}\\ \mathrm{T}^{21} & \mathrm{T}^{22}\end{bmatrix}, \tag{2.52}$$

$$\mathrm{T}^{mn}=\begin{bmatrix}T_{zz}^{mn} & T_{zr}^{mn} & 0\\ T_{rz}^{mn} & T_{rr}^{mn} & 0\\ 0 & 0 & T_{\theta\theta}^{mn}\end{bmatrix},\quad T_{pq}^{mn}=F\,\hat{t}_{pq}^{mn}F^{-1} \tag{2.53}$$

Since scalar elements $\hat{t}_{pq}^{mn}$ of the matrix (2.49) are linear combinations of the plane-wave reflection and transmission coefficients, it is reasonable that we term operator (2.52) as the transmission operator.

2.6. Effective reflection and transmission coefficients

Since in applied problems of geophysics they usually multiply source field traces by the plane-wave coefficients to describe reflection and transmission phenomenon, let us reduce the transmission transform (2.51) to the form of pointwise multiplication.

For that represent the identity matrix as

$$\mathbf{I}=\sum_{\alpha=P,SV,SH}\begin{bmatrix}\mathrm{I}_{\alpha} & 0\\ 0 & \mathrm{I}_{\alpha}\end{bmatrix},\quad \mathrm{I}_{\alpha}=diag\left\{\delta_{\alpha P},\delta_{\alpha SV},\delta_{\alpha SH}\right\}, \tag{2.54}$$

where $\delta_{\alpha\beta}$ is the Kronecker symbol. Substitute the matrix $\mathbf{I}\,\hat{\mathbf{K}}$ instead $\hat{\mathbf{K}}$ into relation (2.49). Then elements (2.53) of the transmission operator (2.52) take the form

$$\mathrm{T}^{mn}=\sum_{\alpha,\beta=P,SV}\mathrm{T}_{\alpha\beta}^{mn}+\mathrm{T}_{SH\,SH}^{mn}, \tag{2.55}$$

where

$$\mathrm{T}^{mn}_{SH\,SH} = F\,\hat{k}^{mn}_{SH\,SH}\,\hat{\mathrm{J}}^{mn}_{SH\,SH}\,F^{-1},\quad \mathrm{T}^{mn}_{\alpha\beta} = F\,\hat{k}^{mn}_{\alpha\beta}\,\hat{\mathrm{J}}^{mn}_{\alpha\beta}\,F^{-1},\quad \alpha,\beta = P, SV, \tag{2.56}$$

$$\begin{aligned}
&\hat{\mathrm{J}}^{mn}_{SH\,SH} = \left(\mathrm{C}\hat{\mathrm{A}}^{+}_{m}\right)\mathrm{I}_{SH\,SH}\left(\mathrm{C}\hat{\mathrm{A}}^{-}_{n}\right)^{-1} = \begin{bmatrix} 0 & 0 & 0 \\ 0 & 0 & 0 \\ 0 & 0 & \hat{J}^{mn}_{SH\,SH,\theta\theta} \end{bmatrix}, \\
&\hat{\mathrm{J}}^{mn}_{\alpha\beta} = \left(\mathrm{C}\hat{\mathrm{A}}^{+}_{m}\right)\mathrm{I}_{\alpha\beta}\left(\mathrm{C}\hat{\mathrm{A}}^{-}_{n}\right)^{-1} = \begin{bmatrix} \hat{J}^{mn}_{\alpha\beta,zz} & \hat{J}^{mn}_{\alpha\beta,zr} & 0 \\ \hat{J}^{mn}_{\alpha\beta,rz} & \hat{J}^{mn}_{\alpha\beta,rr} & 0 \\ 0 & 0 & 0 \end{bmatrix}, \quad \alpha,\beta = P, SV,
\end{aligned} \tag{2.57}$$

$$\mathrm{I}_{SH\,SH} = diag\{0,0,1\},\quad \mathrm{I}_{\alpha\beta} = \left[\delta_{\alpha\gamma}\delta_{\eta\beta}\right],\quad \alpha,\beta,\gamma,\eta = P, SV \tag{2.58}$$

Thus, we introduced operators $\mathrm{T}^{mn}_{\alpha\beta}$ of reflection (when $m = n$) and transmission (when $m \neq n$) for P, SV and SH waves. Obtained form of the operator T^{mn} allows to represent the relation (2.51) in the form of pointwise multiplication

$$\mathbf{v}^{+}\left(\overline{\mathrm{x}}_j\right) = \mathbf{X}\cdot\mathbf{v}^{-}\left(\overline{\mathrm{x}}_j\right), \tag{2.59}$$

where

$$\mathbf{X} = \begin{bmatrix} \mathrm{X}^{11} & \mathrm{X}^{12} \\ \mathrm{X}^{21} & \mathrm{X}^{22} \end{bmatrix},\quad \mathrm{X}^{mn} = \sum_{\alpha,\beta=P,SV} \mathrm{X}^{mn}_{\alpha\beta} + \mathrm{X}^{mn}_{SH\,SH}, \tag{2.60}$$

$$\begin{aligned}
&\mathrm{X}^{mn}_{\alpha\beta} = F\,\hat{k}^{mn}_{\alpha\beta}\hat{\mathrm{J}}^{mn}_{\alpha\beta}F^{-1}diag\left\{\frac{v^{-}_{n,z}\left(\overline{\mathrm{y}}_j\right)}{v^{-}_{n,z}\left(\overline{\mathrm{x}}_j\right)}, \frac{v^{-}_{n,r}\left(\overline{\mathrm{y}}_j\right)}{v^{-}_{n,r}\left(\overline{\mathrm{x}}_j\right)}, 0\right\} = \begin{bmatrix} \chi^{mn}_{\alpha\beta,zz} & \chi^{mn}_{\alpha\beta,zr} & 0 \\ \chi^{mn}_{\alpha\beta,rz} & \chi^{mn}_{\alpha\beta,rr} & 0 \\ 0 & 0 & 0 \end{bmatrix}, \\
&\mathrm{X}^{mn}_{SH\,SH} = \varepsilon_m\varepsilon_n\,F\,\hat{k}^{mn}_{SH\,SH}F^{-1}diag\left\{0,0,\frac{v^{-}_{n,\theta}\left(\overline{\mathrm{y}}_j\right)}{v^{-}_{n,\theta}\left(\overline{\mathrm{x}}_j\right)}\right\} = \begin{bmatrix} 0 & 0 & 0 \\ 0 & 0 & 0 \\ 0 & 0 & \chi^{mn}_{SH\,SH,\theta\theta} \end{bmatrix}
\end{aligned} \tag{2.61}$$

Since each element $\chi^{mn}_{\alpha\beta,\,pq}$ of the matrices (2.61) may be expressed through corresponding plane-wave coefficient $\hat{k}^{mn}_{\alpha\beta}$, we will refer to these functions as effective elastic reflection and transmission coefficients. From the formulas (2.61) it follow that the effective coefficients functionally depend on the normalized source field traces. Therefore we may term the matrix $\mathbf{X}$ as matrix of effective reflection and transmission coefficients. The scheme of action is shown on Fig. 2.2.

Consider behavior of elastic effective coefficients when $kR_n \to \infty$. It is not difficult to show that Lemma 5 from Subsection 1.6 may be generalized for the case of elastic coefficients. We give this result without proof.

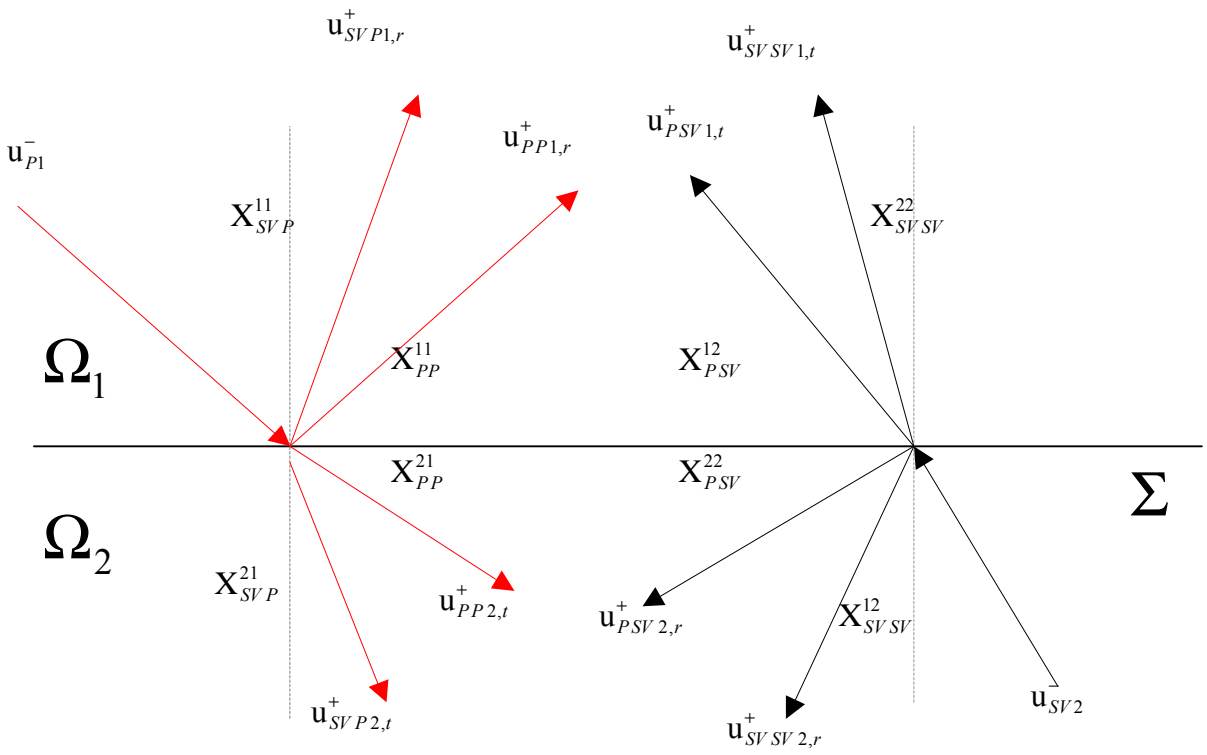


Fig. 2.2. Scheme of action of effective coefficients.

Lemma 6. Coefficients (2.61) tend to corresponding plane-wave coefficients when $kR_n \to \infty$ and the incidence angle γ_n does not coincide with critical angle, i.e.

$$\lim_{kR_n\to\infty} \mathrm{X}^{mn}_{SH\,SH} = \hat{k}^{mn}_{SH\,SH}\ diag\{0,0,1\}, \quad \lim_{kR_n\to\infty} \mathrm{X}^{mn}_{\alpha\beta} = \hat{k}^{mn}_{\alpha\beta}\ diag\{1,1,0\} \tag{2.62}$$

Consider behavior of the effective coefficient of monotype reflection for a point source field of spherical wave and finite values of parameter kh, where $k = \omega\sqrt{c_{P1}^{-2} + c_{S1}^{-2} + c_{P2}^{-2} + c_{S2}^{-2}}$ is mean-square wave number for elastic interface, h is the distance between source and its projection to the interface. Using results of Lemma 6, this coefficient may be compared to corresponding coefficient of the plane wave, which is tangent to the spherical wave at each point. Computations are made for the medium model with typical for seismic waves velocities $c_{P1} = 2\,km/s$, $c_{S1} = 1.2\,km/s$, $c_{P2} = 4\,km/s$, $c_{S2} = 2.4\,km/s$ and density contrast $\rho_1 = 2\,g/cm^3$ and $\rho_2 = 2.6\,g/cm^3$. The only one source is situated in the half-space Ω_1 in the point $(0\,,0\,,1km)$ and generates the longitudinal spherical wave trace at Σ

$$\mathrm{u}_1^-(\bar{\mathrm{x}}_1) = \nabla\frac{\exp\{ik_{P1}\bar{R}\}}{4\pi\bar{R}}, \quad \bar{R} = \sqrt{x_1^2 + x_2^2 + 1} \tag{2.63}$$

On Fig. 2.3 there are the effective reflection coefficients $\chi^{11}_{PP,zz}$ and $\chi^{11}_{PP,rr}$ for various values of the parameter kh: $kh = 10$ (A), $kh = 10^2$ (B), $kh = 10^3$ (C), $kh = 10^4$ (D), $kh \to \infty$ (P).

The graphs show that the effective coefficients essentially depend on the dominant frequency and wave front curvature. This fact may be seen in deviation of the effective coefficient from the plane-wave coefficient in the domain of pure reflection $\gamma_1 < 30^0$. Oscillations of the effective coefficient in overcritical domain ($\gamma_1 > 30^0$) correspond to interference of reflected and two head waves, which are generated at critical incidence angles $\gamma_1^* = 30^0$ and $\gamma_1^* \approx 57^0$. For $\gamma_1 > 57^0$ the unstable oscillations of the effective coefficient are determined by interference of reflected wave and two head waves with different phases. From the graphs it follows that both effective coefficients tend to the same plane-wave coefficient when frequency tends to infinity.

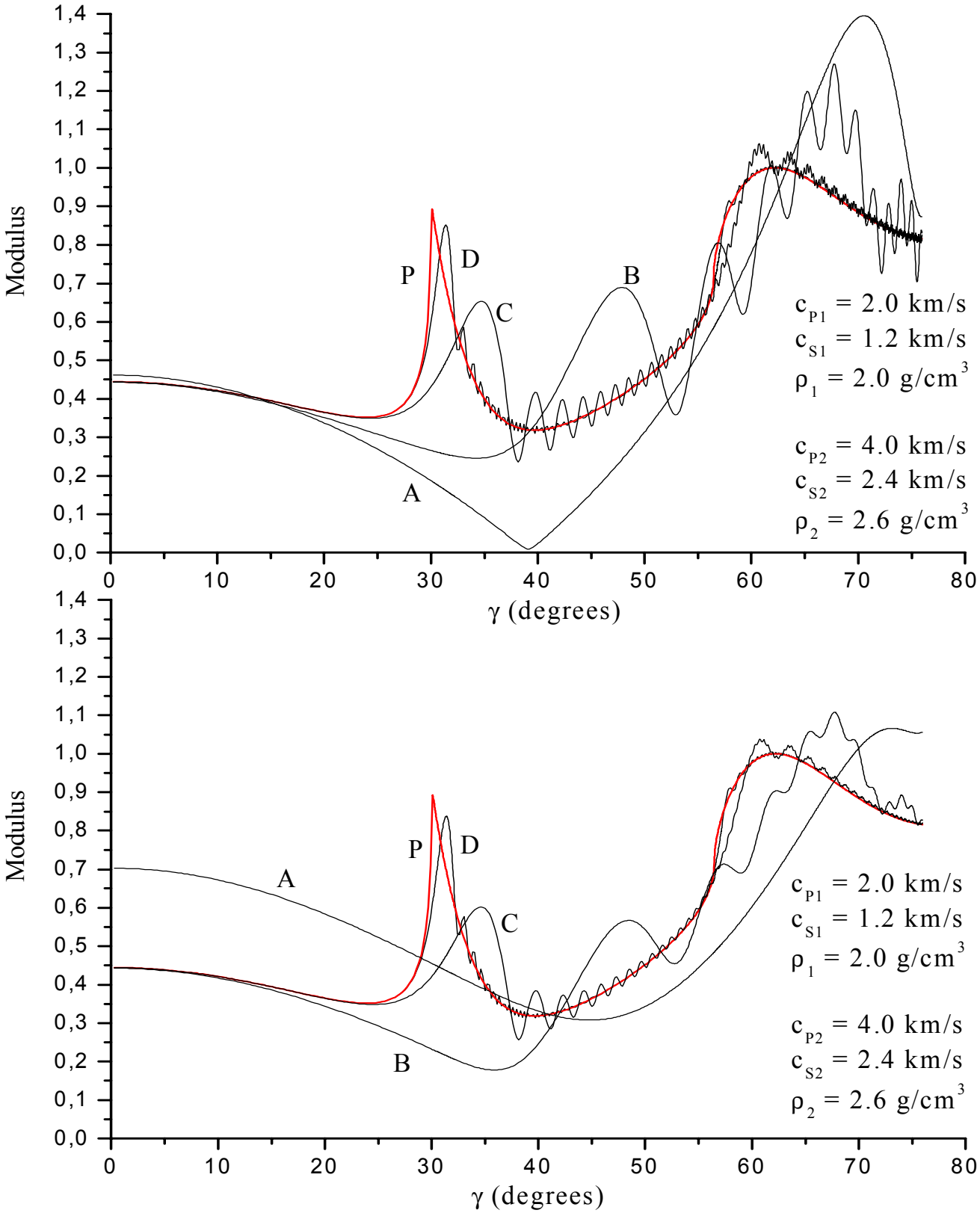


Fig. 2.3. Effective reflection coefficient.

3. SIMULATION OF SCATTERED FIELDS USING EFFECTIVE COEFFICIENTS

In this Section we give examples of exploiting effective coefficients for simulation of scattered fields for acoustic and elastic waves. In Subsection 3.1 we give abstract description of the field, single scattered at curvilinear interface. We give short description of an algorithm for its simulation with help of the Tip Wave Superposition Method (TWSM), which was developed in Institute of Geophysics SB RAS in 80th and 90th and modified by the author with a high-frequency approximation of the effective reflection coefficient (ERC). In Subsection 3.2 we give comparison of synthetic seismograms with the analytic solution for a plane interface and with finite difference and generalized ray solutions for a curvilinear interface in the form of flexure. There introduced synthetic seismograms for anticline interface in the case of concentration of critical points. In Subsection 3.3 we give examples of synthetic seismograms for elastic monotype reflection, scattered at a plane interface for sources of P and SV waves. It is shown that simulation of seismic wave fields with help of elastic ERC allows correct generation not only reflected waves, but also full range of head waves.

3.1. Scheme of modified acoustic version of Tip Wave Superposition Method

Consider stationary transmission problem for scattering of acoustic waves at infinite interface Σ between homogeneous half-spaces Ω_1 and Ω_2. In contrast to the canonical problem (1.1)-(1.3), we assume that the interface Σ is smooth and has the form of a plane with finite curvilinear perturbation. Let the one source be situated in the half-space Ω_1 and generate the spherical wave $u_1^-(\mathrm{x})$. As a result of scattering of the wave $u_1^-(\mathrm{x})$ in each half-space Ω_1 or Ω_2 there arise the wave fields $u_1(\mathrm{x})$ and $u_2(\mathrm{x})$, which are solutions of the problem (1.1)-(1.3) with the transmission conditions given at curvilinear interface Σ. Therefore the vector $\overline{\mathrm{x}}$ is given in curvilinear surface coordinates of Chebyshev type.

In [31] the transmission problem at curvilinear interface is reduced to a vector boundary integral equation for limit values of the field and its normal derivative. The system is modified by introducing the transmission operator that generalizes the operator (1.25). Using results of this work, here we give exact description of the space scattered wave field, single scattered inside Ω_1.

The complete scattered field $u_1^+(\mathrm{x})$ may be represented as [31]

$$u_1^+(\mathrm{x}) = u_1^{+(1)}(\mathrm{x}) + u_1^{+(\infty)}(\mathrm{x}), \quad \mathrm{x} \in \Omega_1, \tag{3.1}$$

where $u_1^{+(1)}(\mathrm{x})$ is single scattered field, $u_1^{+(\infty)}(\mathrm{x})$ is a remainder term, which contains multiple scattering. From (3.1) it follows that, in contrast to the case of plane interface, the reflection process at curvilinear interface contains multiple reflections. However we consider only single scattering $u_1^{+(1)}(\mathrm{x})$.

The single scattered wave field is represented in the form

$$u_1^{+(1)}(\mathrm{x}) = P\left\{r_1^{+(1)}(\overline{\mathrm{x}}_1), \partial r_1^{+(1)}(\overline{\mathrm{x}}_1)/\partial n\right\}, \tag{3.2}$$

where P is a propagation operator in the form of surface Helmholtz integral, $r_1^{+(1)}(\overline{\mathrm{x}}_1)$ is the trace of reflected field, $\partial r_1^{+(1)}(\overline{\mathrm{x}}_1)/\partial n$ is the trace of its normal derivative at interface. Notice that in the case of a plane interface the operator P may be represented in two equivalent forms: in the form of the Weyl-type operator, as in Section 1, or in the form of integral (3.2). In the case of curvilinear interfaces the operator P may be represented only by integral (3.2). The function $r_1^{+(1)}(\overline{\mathrm{x}}_1)$ in the formula (3.2) describes trace of the wave field, locally reflected at the point $\overline{\mathrm{x}}_1 \in \Sigma$. The single scattered field $u_1^{+(1)}(\mathrm{x})$ represents interference of separate wave fragments coming from various points of the interface Σ.

The values $r_1^{+(1)}(\overline{\mathrm{x}}_1)$ and $\partial r_1^{+(1)}(\overline{\mathrm{x}}_1)/\partial n$ in arbitrary fixed point $\overline{\mathrm{x}}_1 \in \Sigma$ may be expressed through the source field trace $u_1^-(\overline{\mathrm{x}}_1)$ and its normal derivative $\partial u_1^-(\overline{\mathrm{x}}_1)/\partial n$ as

$$\begin{aligned} r_1^{+(1)}(\overline{\mathrm{x}}_1) &= K_{11}\, u_1^-(\overline{\mathrm{y}}_1), \\ \partial r_1^{+(1)}(\overline{\mathrm{x}}_1)/\partial n &= -K_{11}\, \partial u_1^-(\overline{\mathrm{y}}_1)/\partial n, \end{aligned} \tag{3.3}$$

where the integral transmission operator K_{11} is defined by the relation (1.26) and has the form of convolution in curvilinear surface coordinates.

For approximate description of the field (3.2), the author used the acoustic version of the TWSM algorithm [11, 12, 32]

$$\tilde{u}_1^{+(1)}(\mathrm{x}) = \tilde{P}\, \tilde{r}_1^{+(1)}(\overline{\mathrm{x}}_1), \tag{3.4}$$

where $\tilde{P}$ is a high-frequency approximation of the propagation operator P. To compute the trace (3.3) in the TWSM they used an approximate formula $\tilde{r}_1^{+(1)}(\overline{\mathrm{x}}_1) = \chi_{11}(\infty)\, u_1^-(\overline{\mathrm{x}}_1)$ with the plane-wave reflection coefficient $\chi_{11}(\infty)$ [12]. Since the coefficient $\chi_{11}(\infty)$ generates essential artefacts, we included a high-frequency approximation of the ERC $\tilde{\chi}_{11}$ instead of $\chi_{11}(\infty)$ in the TWSM. At that, the single reflected field trace may be represented as [10]

$$\tilde{r}_1^{+(1)}(\overline{\mathrm{x}}_1) = \tilde{\chi}_{11}\, u_1^-(\overline{\mathrm{x}}_1) \tag{3.5}$$

In accordance to the agreed asymptotical approximation (3.4)-(3.5), the exact single scattered filed is

$$u_1^{+(1)}(\mathrm{x}) = \tilde{u}_1^{+(1)}(\mathrm{x}) + \Delta_{TWSM} u_1^{+(1)}(\mathrm{x}) + \Delta_{EC} u_1^{+(1)}(\mathrm{x}), \tag{3.6}$$

where $\Delta_{TWSM} u_1^{+(1)}(\mathrm{x})$ and $\Delta_{EC} u_1^{+(1)}(\mathrm{x})$ are mistakes in computation of the space scattered field due to introduction of $\tilde{P}$ and $\tilde{\chi}_{11}$ correspondingly. Only in the case of plane interface the relation $\Delta_{EC} u_1^{+(1)}(\mathrm{x}) = 0$ holds true due to the property $\tilde{\chi}_{11} = \chi_{11}$.

In applied problems of seismics to describe phenomena at interfaces in formula (3.5) they usually use the plane-wave reflection coefficient instead of ERC. By definition, the plane-wave coefficient does not take into consideration the wave front curvature and, as a consequence, does not allow generation of head waves, which have essential meaning for data processing. Moreover, as it was shown in Subsection 1.5, this coefficient belongs to the Hölder class. Therefore the trace (3.5) computed with help the plane-wave coefficient does not belong to the class of continuously differentiable functions. Consequently, the necessary condition of existence of normal derivative of the integral (3.2) for derivation the boundary integral equation in [31] is violated [20]. As a result, the scattered field contains diffraction artefacts generated in the breaking points of the plane-wave reflection coefficient. It is known that any method based on Helmholtz surface integrals and plane-wave coefficients generates artefacts of that type [38; 41]. Therefore the plane-wave coefficient is not sufficient to simulate reflected wave fields in terms of surface integrals. Exploiting the effective coefficient allows removing mentioned artefacts and adding head waves to obtain more complete and realistic seismic wave field.

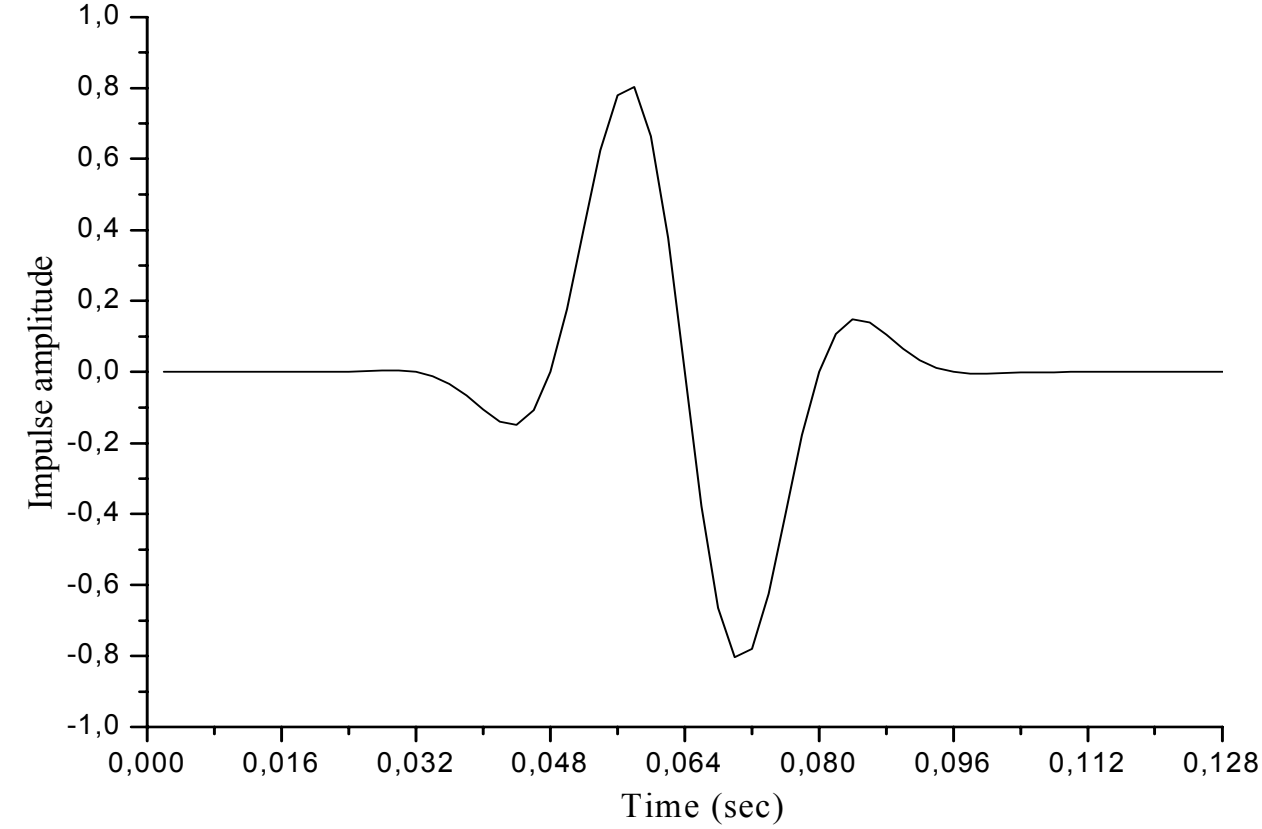
3.2. Acoustic wave field, single scattered at curvilinear interface

Let us demonstrate the opportunities of the effective coefficients on examples of simulation of nonstationary single reflected wave fields with help of the TWSM [10]. Simulations are carried out in the domain of time frequency ω with the later application of the standard algorithm of the fast Fourier transform. In all the tests we use the impulse form (Fig. 3.1)

$$F(t) = -\exp\left(-p^2/\pi^2\right)\sin(p), \quad p = 2\pi\frac{(t-t_0)}{T}, \tag{3.7}$$

where $t_0 = 0.064c$ is a time shift for the central point of the impulse, $T = 0.032c$ is the wave period.

In accordance to traditions in seismics, the synthetic space wave fields are shown as seismograms, which are section of the wave field on the plane (t, x_1). Parameter t is continuous on the interval $(t_{\min}, t_{\max})$ of the abscissa axis, parameter x_1 is discrete and given on the interval $(x_{\min}, x_{\max})$ of the ordinate axis.



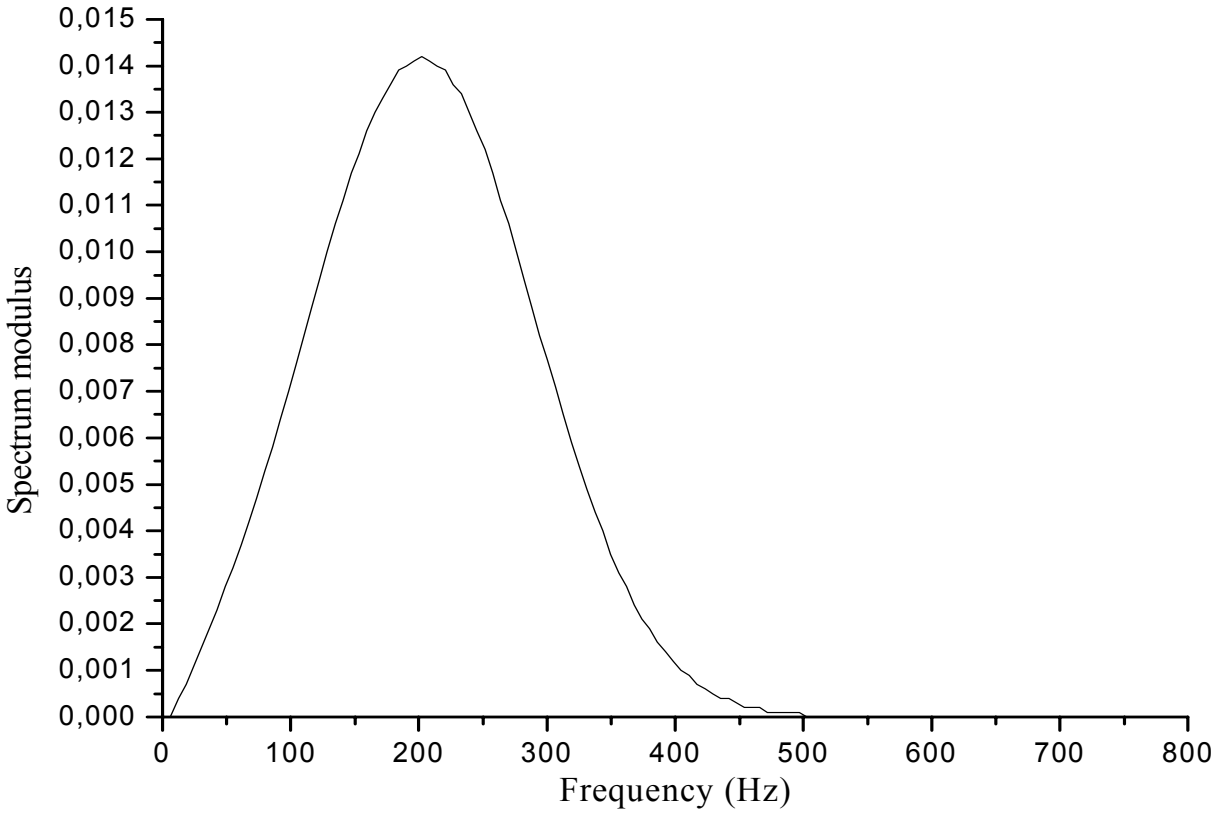


Fig. 3.1. Impulse and its spectrum.

Test 1. The first test is carried out for a plane interface since in this case the mistake $\Delta_{EC}u_1^{+(1)}(\mathrm{x})$ is absent. This fact gives possibility to evaluate the accuracy of the TWSM algorithm. At that, we can simulate the exact space scattered field by the formulas (1.15) and (1.24). Therefore we can compare the approximate TWSM solution and the exact solution.

Let us assume the point source of the spherical wave be situated in the point with coordinates $(0,0,1km)$. Comparison of the TWSM algorithm with the exact simulation is made for an interface given by the equation $x_3 = 0$. Let the density contrast be absent, i.e. $\beta = \rho_1/\rho_2 = 1$, and the velocities be $c_1 = 2km/s$, $c_2 = 4km/s$. We consider the single scattered field (3.4) in the points $(x_1,0,1km)$, where $x_1 = k\Delta x_1$, $\Delta x_1 = 0.05km$, $k \in [0,58] \subset N$ (Fig. 3.2).

It is necessary to notice that in the case of a plane horizontal interface between homogeneous half-spaces kinematical part of the problem may be described by enough simple formulas. At first, for a point source the locus of head wave generation is a circle with the center in the source projection point and is defined by the Snell's law

$$\frac{\sin\gamma_1}{c_1} = \frac{\sin\gamma_2}{c_2}, \tag{3.8}$$

where γ_j is the incidence or reflection angle in the half-space Ω_j. Consider, for example, the contrast $c_1 < c_2$, which we will use for all the tests below. From the formula (3.8) it follows that for the incidence angle γ_1^* such that $\sin\gamma_1^* = c_1/c_2$ the relation $\sin\gamma_2^* = 1$ holds true. The angle γ_1^* is the critical incidence angle. Corresponding points on the interface coincide with the points where the reflection coefficient is not smooth. For all angles $\gamma_2 > \gamma_2^*$, front of the transmitted wave in the half-space Ω_2 propagates along the interface. Since $c_1 < c_2$, for all $\gamma_1 > \gamma_1^*$, front of the transmitted wave passes ahead of the reflected wave front. Therefore there appears discontinuity of the wave field at the interface. Head wave arises as smoothing correction that compensates this discontinuity and has the form of a wave with conical front tangent to the reflected wave front.

Secondly, it is easy to calculate the arrival time of reflected and head waves on the profile. For the considered model the reflected wave arrival time is given by the formula $\tau_r(x_1) = \sqrt{4h^2 + x_1^2}/c_1$, the head wave arrival time is $\tau_H(x_1) = \tau_H^* + (x_1 - x_1^*)/c_1$, where $\tau_H^* = 2h/(c_1\cos\gamma_1^*)$, $x_1^* = 2h\,\mathrm{tg}\,\gamma_1^*$, h is the distance between source and point of its projection on the interface. These two kinematic wave properties allow controlling accuracy of computations.

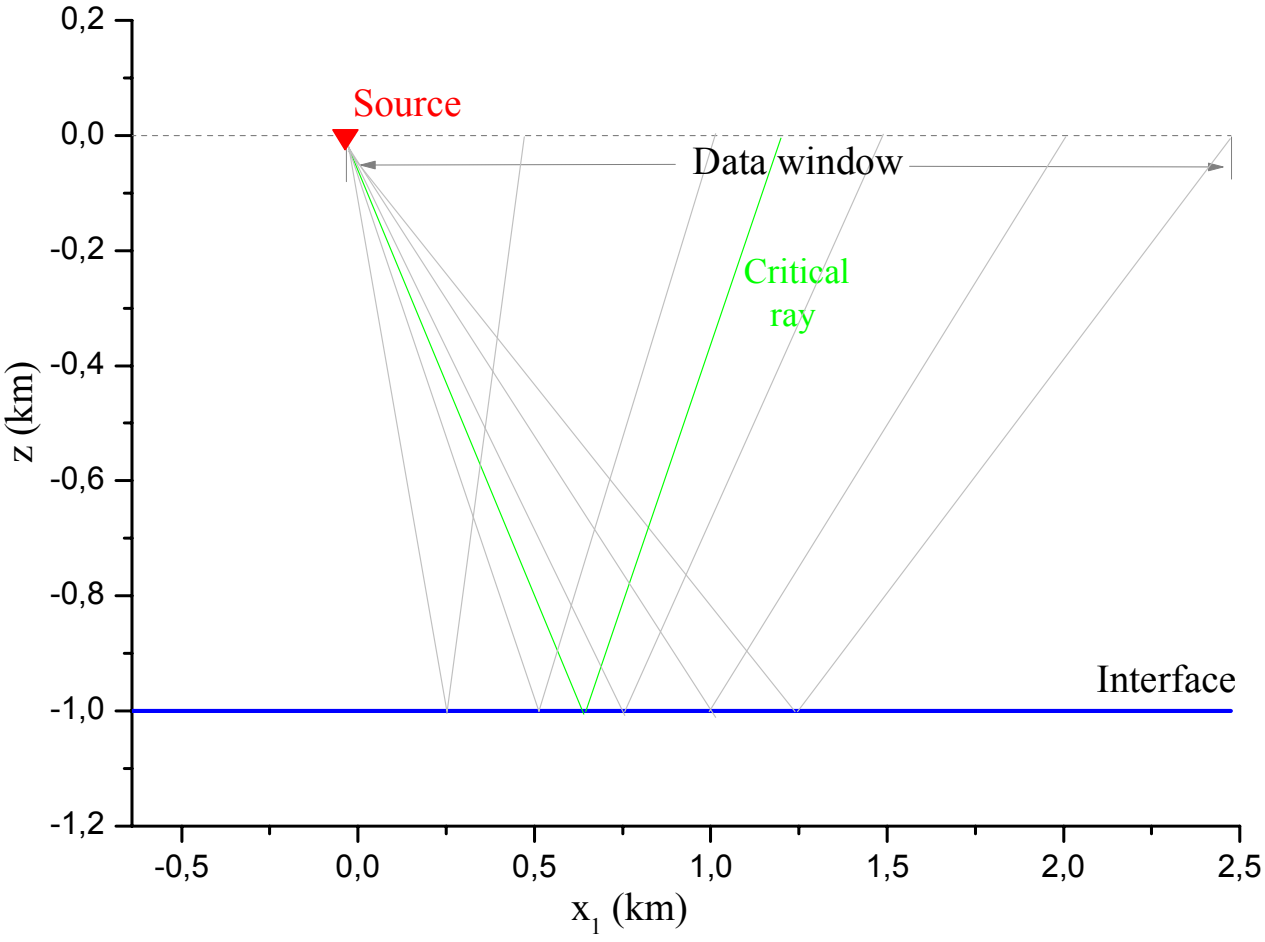


Fig. 3.2. Medium model.

On Fig. 3.3 we give two seismograms computed with help of the TWSM. The first seismogram is simulated with the plane-wave reflection coefficient. From the graph it follows that, in addition to reflected wave, the seismogram contains artificial diffracted wave generated by a circle of critical points on the interface. Second seismogram is simulated with help of ERC. On this seismogram there are only reflected wave with hyperbolic hodograph curve and head wave with straight hodograph curve. The above-mentioned artefact is removed.

Estimate accuracy of the TWSM algorithm. On Fig. 3.4 we give two seismograms: exact seismogram (red) and TWSM seismogram (black). Since the ratio error of the TWSM does not exceed adequate value of several percents, the difference between TWSM and exact seismograms is not evident. Therefore on Fig. 3.5 we give detailed comparison for three separated traces: 1) zone of subcritical reflection at $x_1 = 0$; 2) zone of interference of reflected and head waves at $x_1 = 1.55\,km$; 3) zone of overcritical reflection at $x_1 = 2.55\,km$. The graphs also have small differences. Therefore we can maintain that the TWSM with ERC allows simulation of synthetic wave fields with high degree of accuracy.

Test 2. For the case of curvilinear interface comparison of the TWSM seismograms and exact seismograms cannot be realized yet since for computation of single scattered field we need to realize the propagation operator in the formula (3.2) and the reflection operator in the interface curvilinear coordinates in (3.3). Therefore we made comparison of the TWSM seismograms with seismograms obtained by essentially another methods: the generalized ray and finite difference seismograms from [27]. In the work they consider the medium model as follows. The wave propagation velocities are $c_1 = 3\,km/s$ and $c_2 = 4\,km/s$. The interface has form of flexure given by the equation $x_3 = -0.185 + 0.2\,\tanh\{2\pi(x_1 - 2)\}\,km$. In the work they give seismograms of vertical component of single scattered elastic field for the profile, distributed between $(-0.75\,km, 0, 0.415\,km)$ and $(1.25\,km, 0, 0.415\,km)$. Receivers are distributed with the interval $\Delta x_1 = 0.02\,km$. Fig. 3.6 shows the medium model and data window. Both synthetic seismograms contain single reflection in the form of caustic. Notice that the head wave is absent since it cannot be registered by the chosen profile. In this Test acoustic TWSM seismograms were computed using the plane-wave reflection coefficient and ERC. These seismograms are shown on Fig. 3.7. On the TWSM seismogram we observe reflection in the form of caustic, which is conditioned by the relief of reflector. The first seismogram is essentially distorted by a diffraction artefact generated by contour of critical points at the interface. On the second seismogram, which is computed using ERC, this artefact is absent. Although for simulation we used acoustic version of the TWSM, second seismogram shows qualitative coincidence with seismograms of components from [27].

Test 3. This test is made to control steadiness of reproduction of the head wave field, which is generated at curvilinear interface, when simulating with help of TWSM and ERC. For that we consider an anticline interface, which is chosen so that there appears a wide strip of several critical contours. Let the interface be given by the expression $x_3 = -1 + 0.1\exp\{-16(x_1^2 + x_2^2)\}\,km$ (Fig. 3.8). The wave propagation velocities are $c_1 = 2\,km/s$ and $c_2 = 4\,km/s$. The profile is situated between points $(0, 0, 1\,km)$ and $(2\,km, 0, 1\,km)$. The receivers are distributed with the interval $\Delta x_1 = 0.02\,km$.

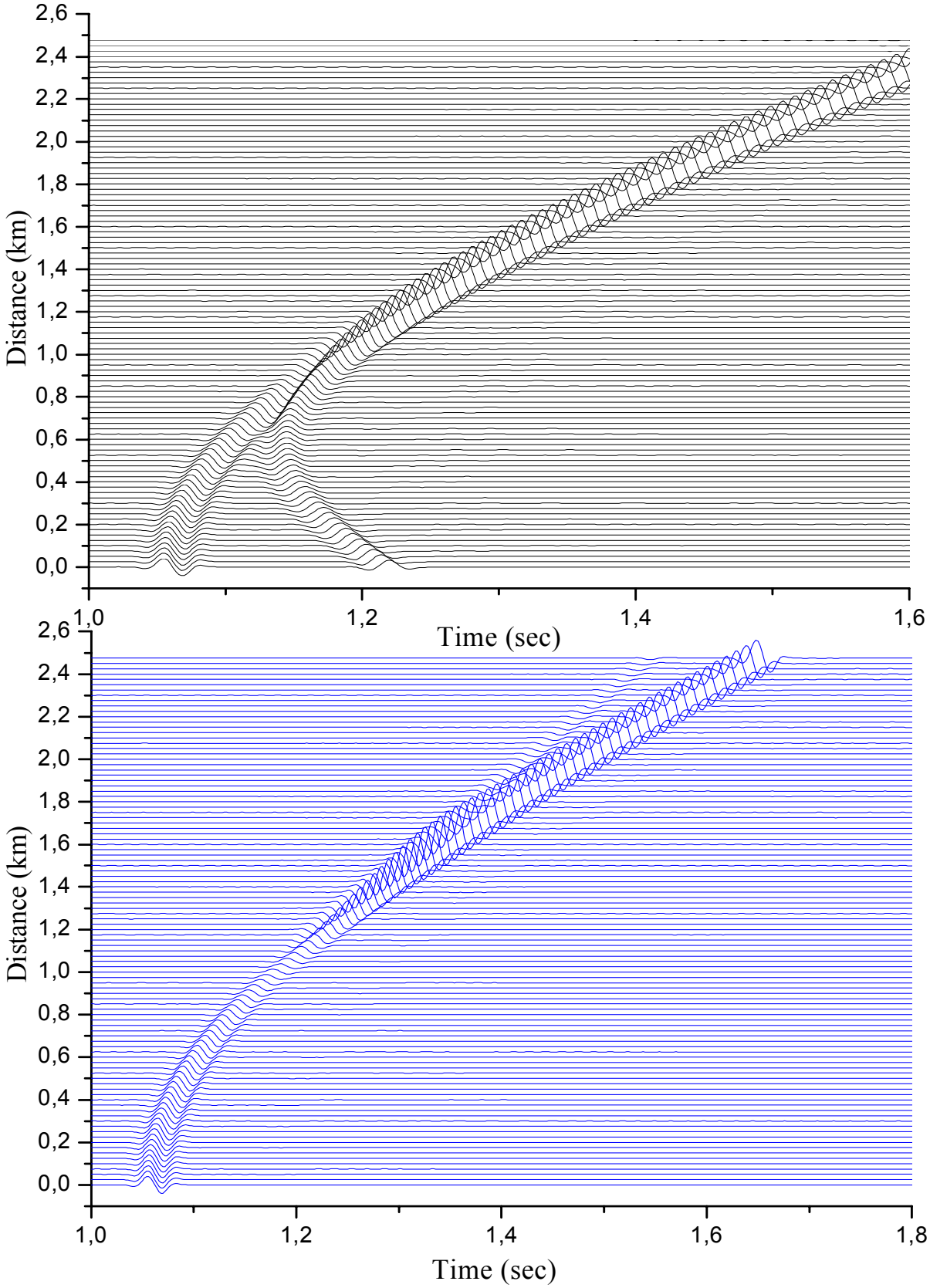


Fig. 3.3. TWSM seismograms.

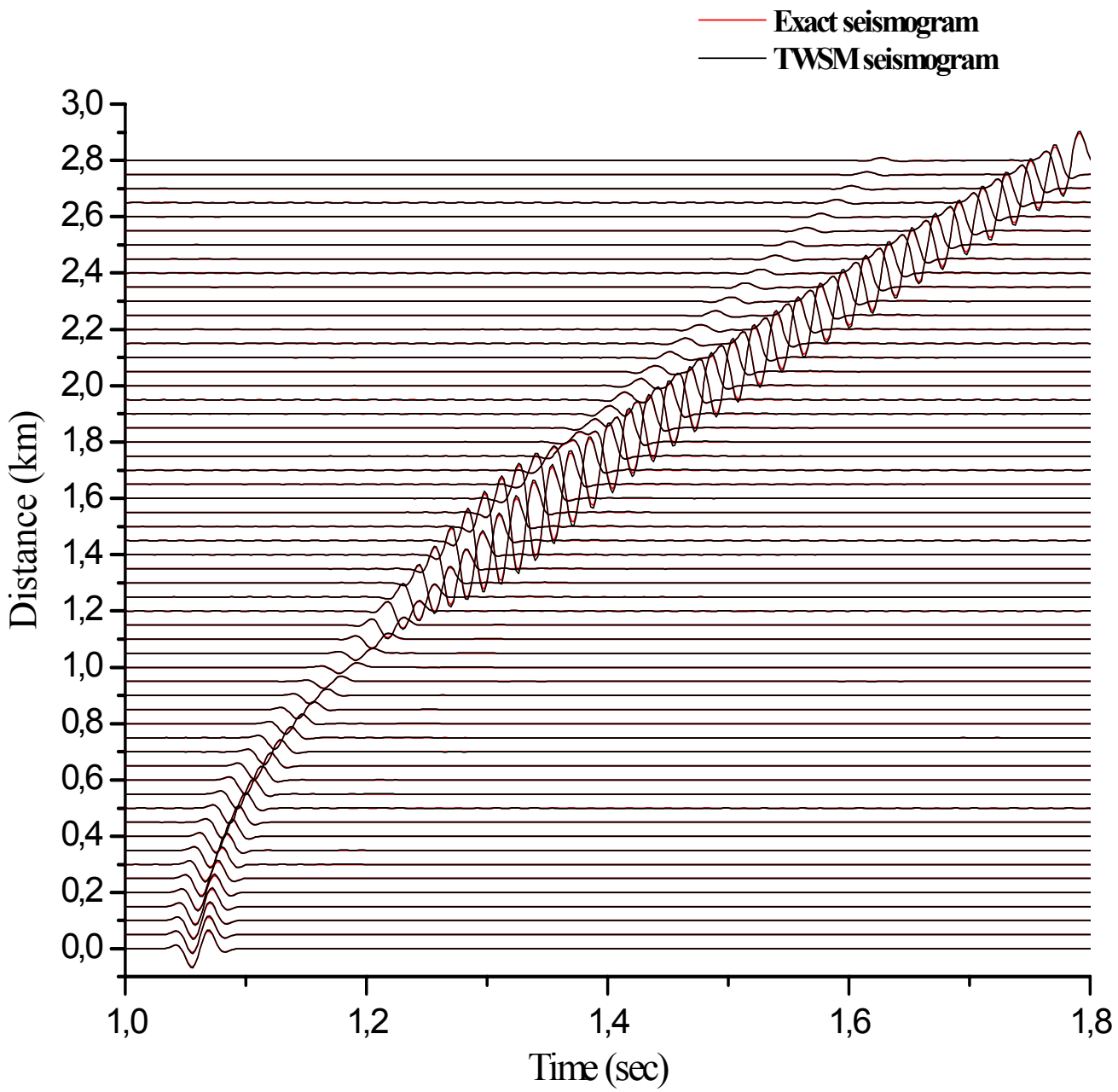


Fig. 3.4. Comparison of TWSM seismogram with exact solution.

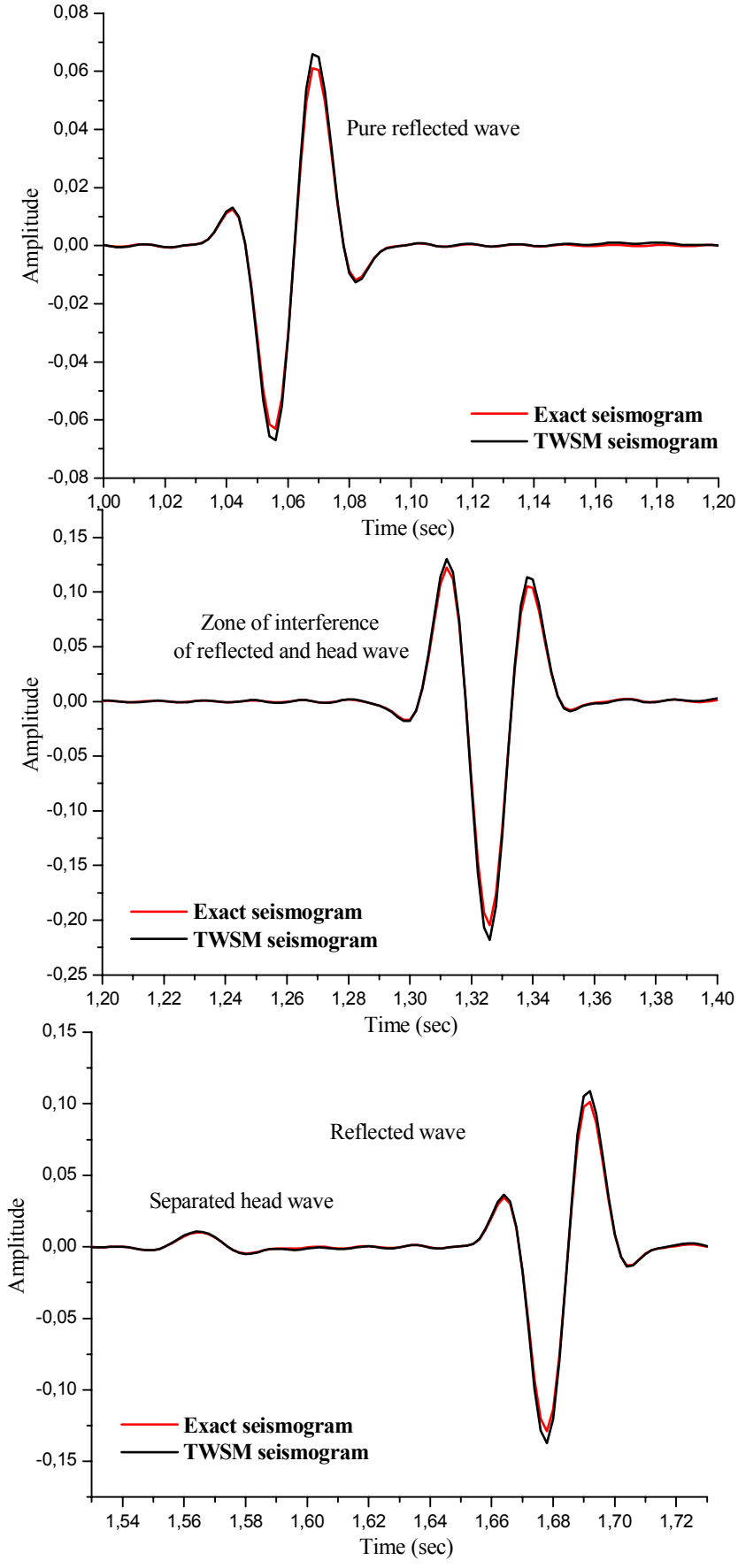


Fig. 3.5. Comparison of TWSM seismograms with exact solution.

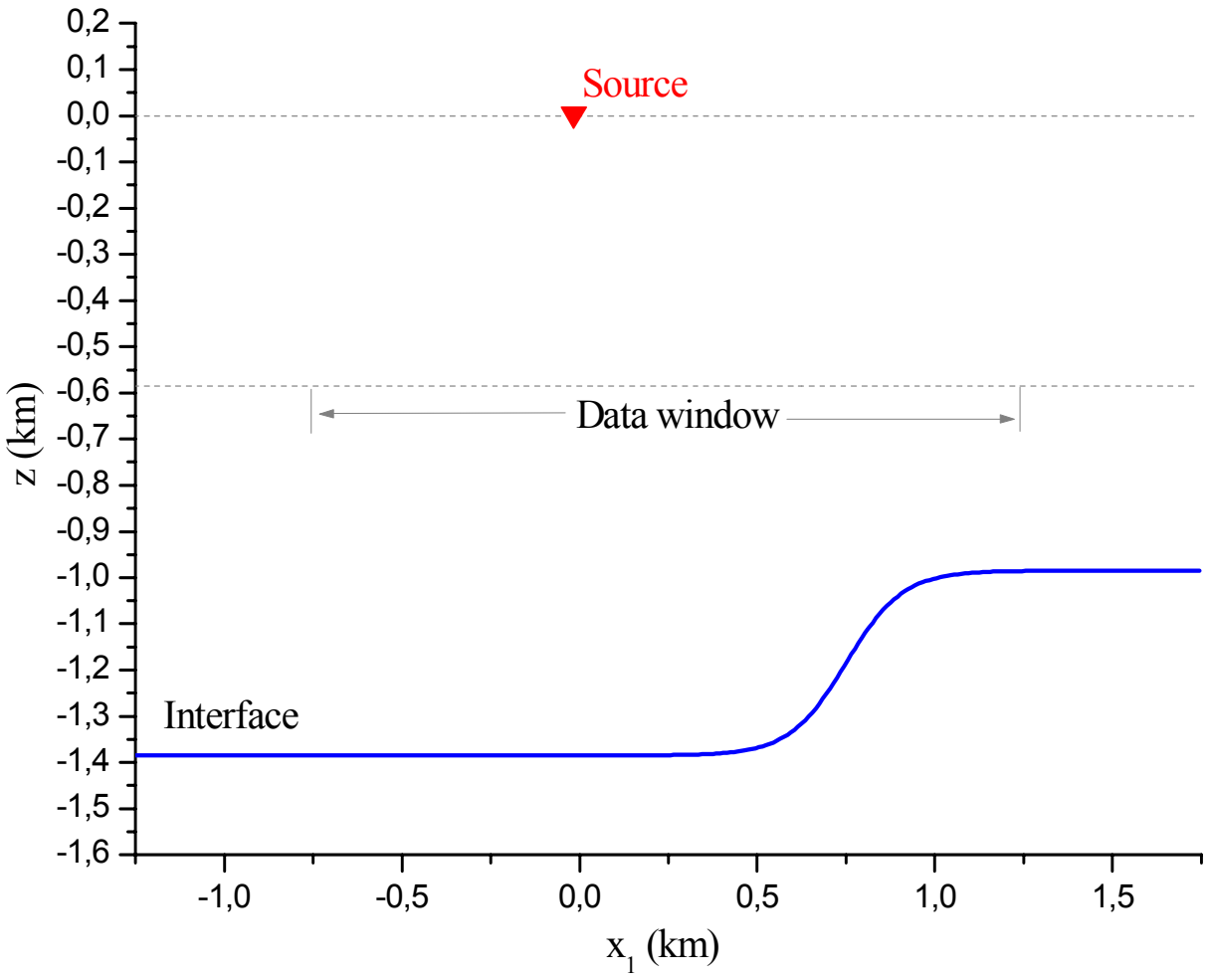


Fig. 3.6. Medium model.

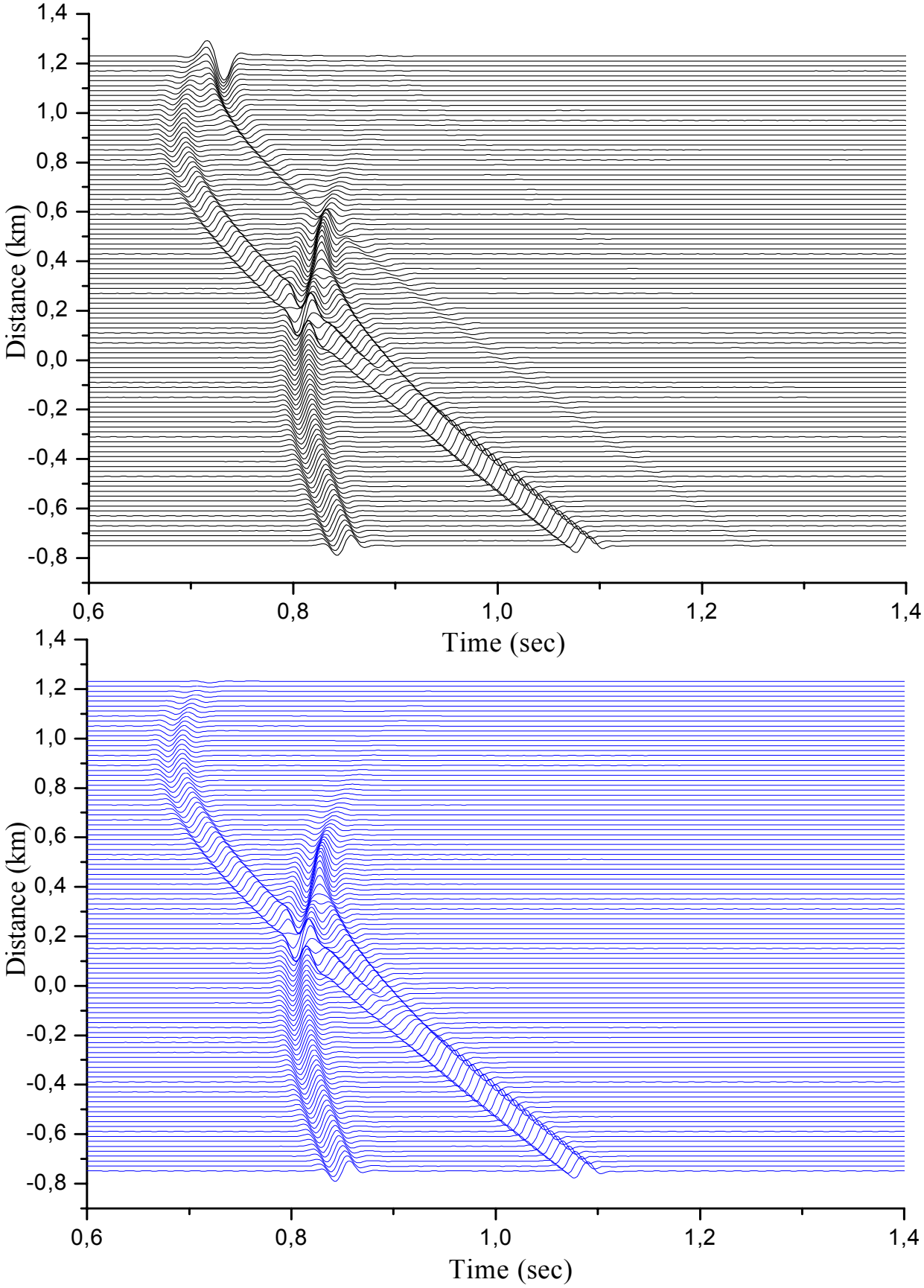


Fig. 3.7. TWSM seismograms.

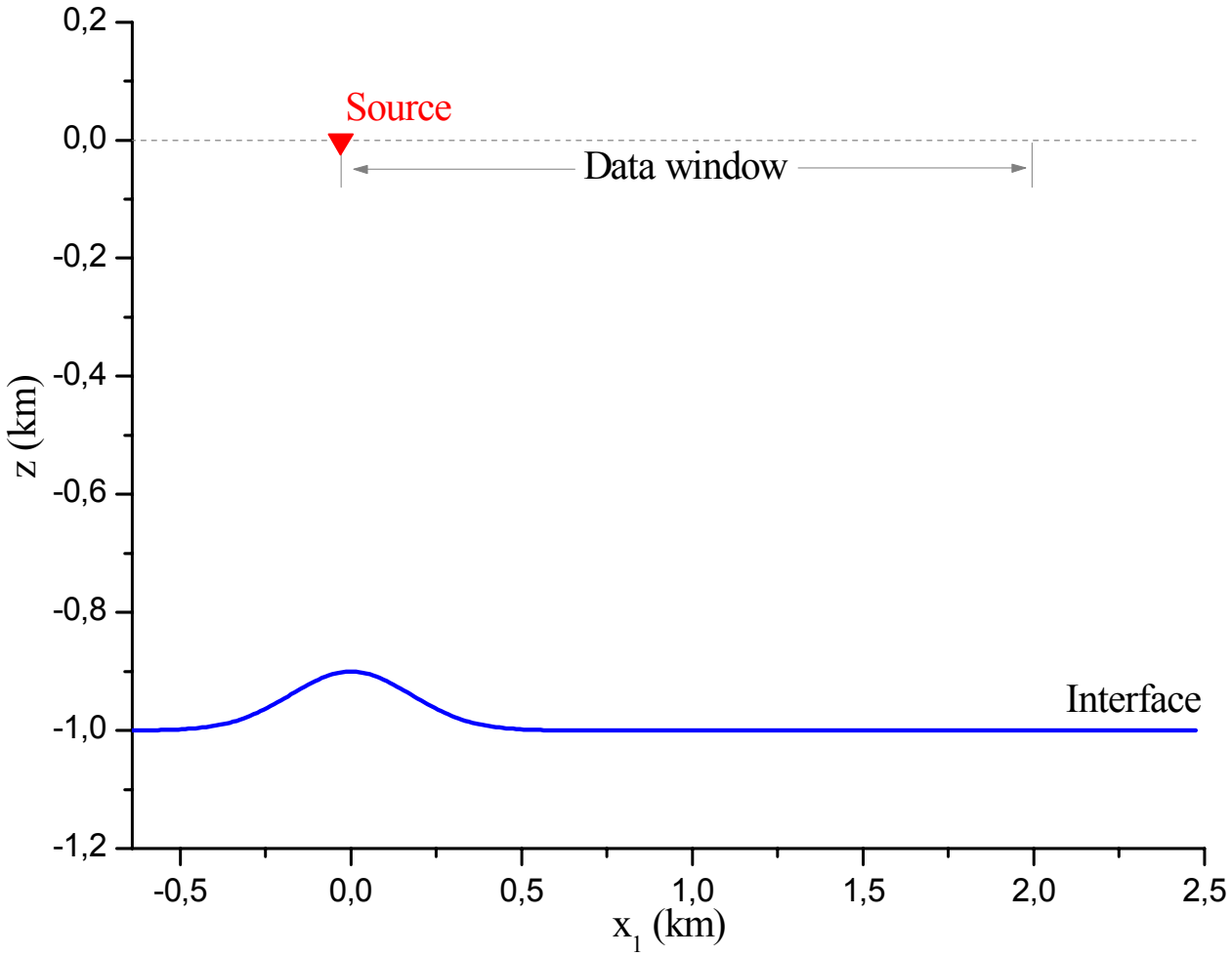


Fig. 3.8. Medium model.

At the interface there are three critical circles with radiuses $0.185\,km$, $0.29\,km$ and $0.566\,km$, and centers coinciding with the projection of source on the interface. Both TWSM seismograms contain reflection with almost hyperbolic hodograph (Fig. 3.9). The seismogram, obtained with help of the plane-wave reflection coefficient, contains three diffraction artefacts, which essentially distort the wave field. On the seismogram computed with ERC these artefacts are absent. Moreover, we can observe two head waves: one from the critical circle with radius $0.566\,km$ at plane part of the interface, as in Test 1, "slow" head wave from the strip with the internal radius $0.185\,km$ and external radius $0.29\,km$ at curvilinear part of the interface. "Slow" head wave has apparent velocity lower than velocity of reflected wave since is arrives from the anticline part to the distant part of profile under sharp angle. In the central part of the profile we observe weak caustic generated by concave part of anticline.

3.3. Elastic wave field scattered at plane interface

Below we give results of first tests on simulation nonstationary elastic scattered wave fields for the case of plane interface between two homogeneous half-spaces. These fields are computed in ω domain with help of formulas (2.28), (2.47) and (2.51) with implementation of the fast Fourier transform algorithm. Two tests are given to control steadiness of generation of monotype reflected wave and full range of head waves when using ERC.

Test 4. Let the source be situated in the point $(0,0,1km)$ of the half-space Ω_1 (Fig. 3.2). It generates the longitudinal spherical wave

$$\mathrm{u}_1^-(\mathrm{x}) = \nabla \frac{\exp\{ik_{P1}R\}}{4\pi R}, \tag{3.9}$$

where $R = \sqrt{x_1^2 + x_2^2 + (x_3 - 1)^2}$. In Ω_1 the wave propagation velocities are $c_{P1} = 2\,km/s$ and $c_{S1} = 1.2\,km/s$ and density is $\rho_1 = 2\,g/cm^3$, in Ω_2 the wave propagation velocities are $c_{P2} = 4\,km/s$ and $c_{S2} = 2.4\,km/s$ and density is $\rho_2 = 2.6\,g/cm^3$. The interface Σ is given be the expression $x_3 = 0$. The profile is situated between points $(0,0,1km)$ and $(2km,0,1km)$. Receivers are situated at the interval $\Delta x_1 = 0.02\,km$.

Notice that for elastic half-spaces the Snell's law has the form

$$\frac{\sin\gamma_{P1}}{c_{P1}} = \frac{\sin\gamma_{S1}}{c_{S1}} = \frac{\sin\gamma_{P2}}{c_{P2}} = \frac{\sin\gamma_{S2}}{c_{S2}}, \tag{3.10}$$

where $\gamma_{\alpha j}$ is the incidence or reflection angle of α-type wave in Ω_j. From (3.10) it follows that for the chosen velocities for a longitudinal incident wave in Ω_1 there are two head waves in the reflected field [19]. The first one, conditioned by contrast c_{P1}/c_{P2}, has smaller arrival times. The second one, corresponding to c_{P1}/c_{S2}, arrives later and has weaker amplitude.

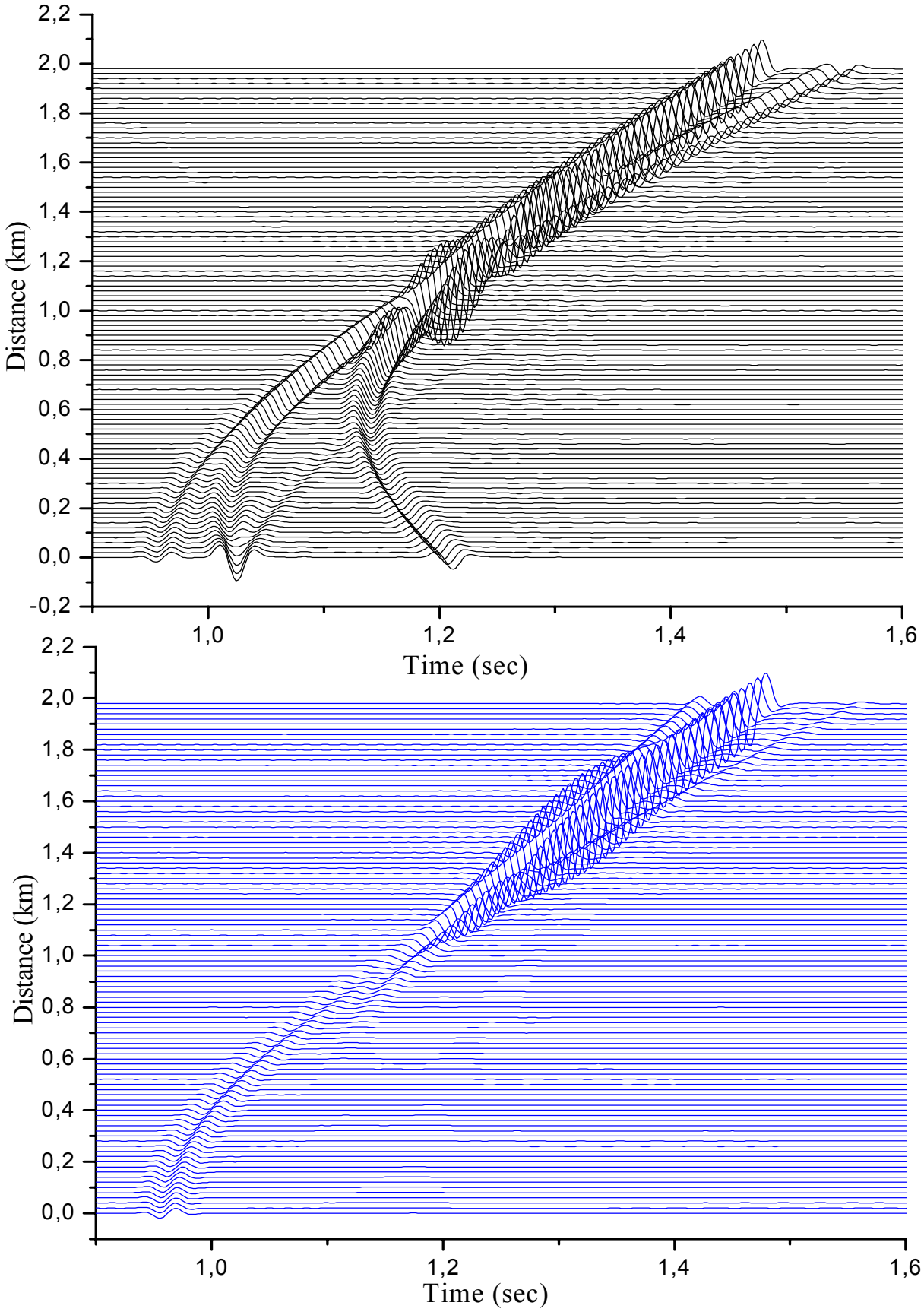


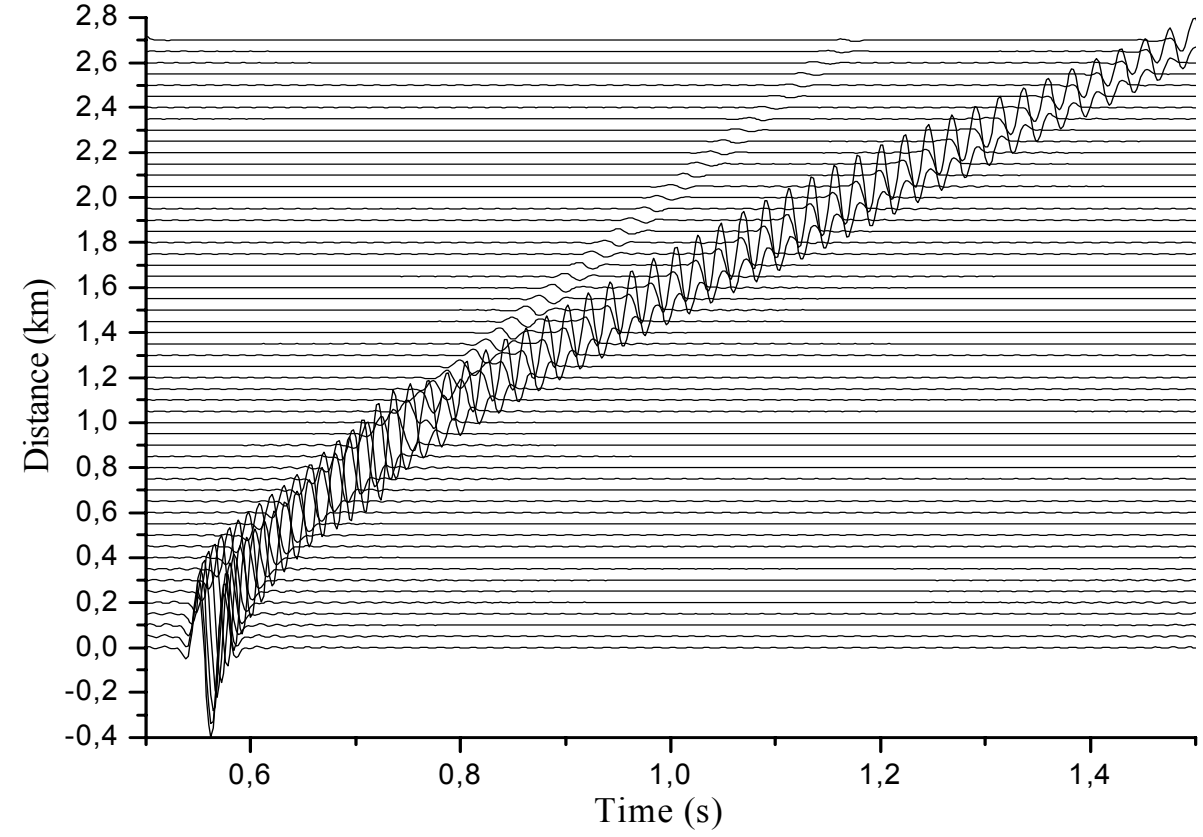
Fig. 3.9. TWSM seismograms.

On Fig. 3.10 we give exact seismogram for vertical component of monotype longitudinal wave field scattered at plane interface. On the seismogram we observe reflected wave and two above-mentioned head waves. Since the head waves have weaker amplitudes than reflected wave, we give reduced seismogram. On this seismogram the reflected wave hodograph is reduced to the straight line.

Test 5. Let the SV wave source be situated in the point $(0,0,1km)$ of the half-space Ω_1 (Fig. 3.2). It generates the wave

$$\mathrm{u}_1^-(\mathrm{x}) = \nabla\times\left(0,0,\frac{\exp\{ik_{P1}R\}}{4\pi R}\right), \tag{3.11}$$

where $R=\sqrt{x_1^2+x_2^2+(x_3-1)^2}$. The medium model, interface and data window are the same as in Test 4. On Fig. 3.11 we give exact seismogram of horizontal component of monotype wave field scattered at plane interface. On the seismogram we observe reflected SV wave and three corresponding head waves. The number of head waves is determined by the Snell's law (3.10) and corresponds to three velocity contrasts: c_{S1}/c_{P2}, c_{S1}/c_{S2} and c_{S1}/c_{P1} [19]. Also we give reduced seismogram that confirms existence of full range of head waves.



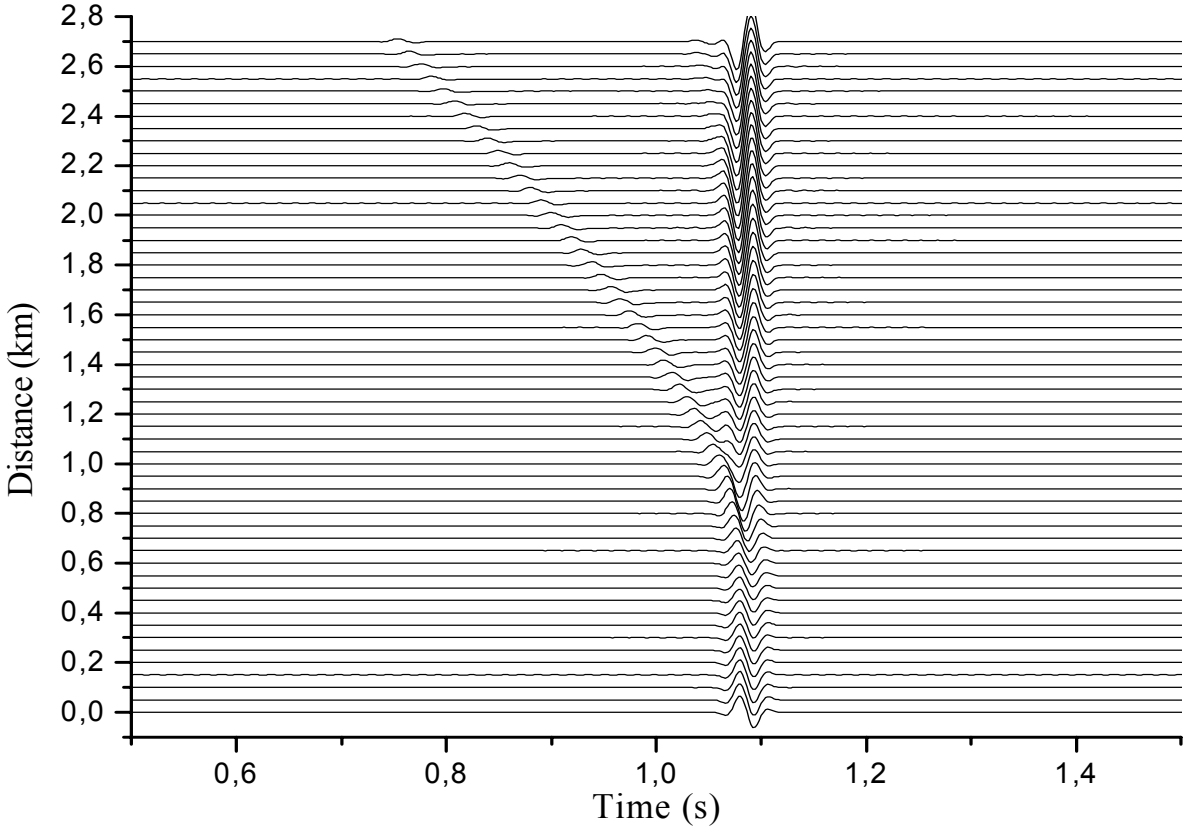


Fig. 3.10. Vertical component of P-P wave.

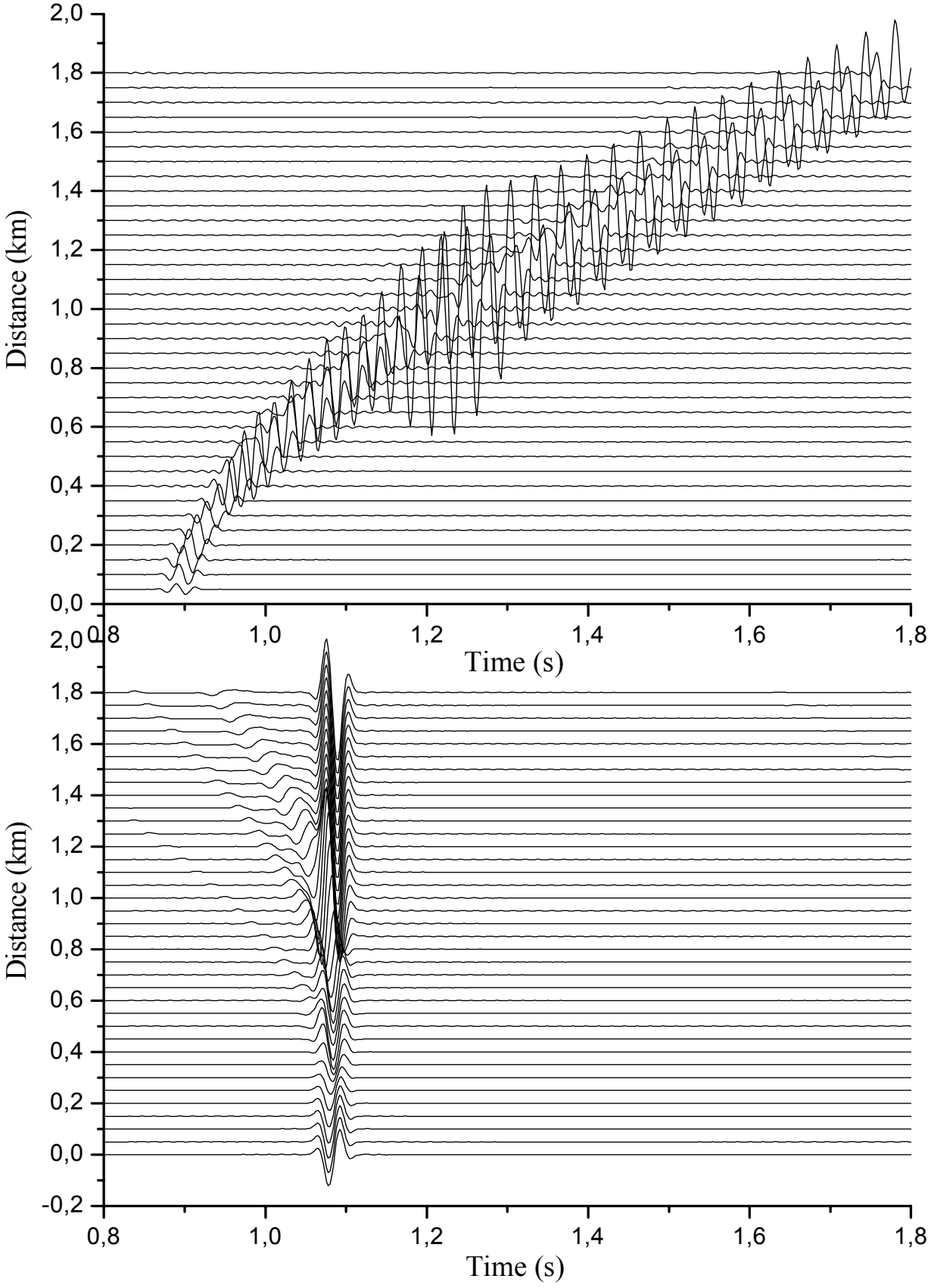


Fig. 3.11. Horizontal component of SV-SV wave.

CONCLUSIONS

Basic results of the thesis are:

1. Known solution of the canonical transmission problems for acoustic and scalar waves are represented as result of action of propagation and transmission operators composition over the source field trace at the interface.

2. Scalar elements of the transmission operator are expressed through the integral reflection and transmission operators in the form of convolutions over the interface with the kernels containing the plane-wave reflection and transmission coefficients.

3. The reflection and transmission operators are represented in the form of effective (functional) coefficients. It is shown that the effective coefficients tend to corresponding plane-wave coefficients when the frequency tendes to infinity.

4. The stable algorithms for numerical realization of effective acoustic and elastic coefficients are developed.

5. With help of simulation of single scattered wave field by TWSM it is shown that application of the effective coefficients allows correct and enough accurate simulation of reflected waves as well as head waves.

First and second results for acoustic waves are obtained by the author but represent particular case of common transmission problem at curvilinear interface [31]. These results for elastic waves, as well as third, fourth and fifth results, are new and obtained by the author.

Based on the obtained results, the author plans to include elastic effective coefficients in the elastic version of TWSM. In the outlook, we can expect that: 1) usage of effective coefficients for simulation scattered wave fields with help of surface propagators will improve the quality of synthetic wave fields; 2) inclusion of effective coefficients into algorithms for solving inverse problems of seismics will improve their abilities.

In conclusion, the author thanks her scientific supervisors: the project leader professor Kamill D. Klem-Musatov for the possibility to work in the new and interesting research area and doctor Vladimir A. Tcheverda for the help in making-ready the thesis. The author takes the opportunity to express her thanks to doctor Arkady M. Aizenberg for useful comments during the research and to doctors Hans B. Helle and Jan Pajchel for consultations on numerical technology and possibility of testing TWSM on powerful computers.

REFERENCES

1. Aizenberg M.A. Research of properties of the reflection/transmission operator in transmission problem at plane interface between two homogeneous half-spaces. Materials of 39th International Scientific Conference for Students "Student and Scientific-Technical Progress", Mathematics, Differential equations. Novosibirsk State University, Novosibirsk, 2001, 134-135 (in Russian).

2. Aizenberg M.A. Research of properties of the reflection/transmission operator in transmission problem at plane interface between two homogeneous half-spaces. International Conference of Young Scientists, Specialists and Students "Geophysics 2001", Thesis of presentations, Novosibirsk, Academgorodok, 94-95 (in Russian).

3. Aizenberg M.A. Research of properties of the transmission operator in transmission problem at a plane interface between two homogeneous half-spaces. Geophysical Bulletin of EAGO, 2002, 1, 10-12 (in Russian).

4. Aizenberg M.A. Research of properties of the transmission operator in the reflection/transmission problem at plane interface between two homogeneous half-spaces. Materials of 40th International Scientific Conference for Students "Student and Scientific-Technical Progress", Mathematics, Differential equations. Novosibirsk State University, Novosibirsk, 2002, 24 (in Russian).

5. Aizenberg M.A. Simulation of interference wave field trace reflected by plane interface of two homogeneous media. Materials of 40th International Scientific Conference for Students "Student and Scientific-Technical Progress", Geology, Geophysics. Novosibirsk State University, Novosibirsk, 2002, 78 (in Russian).

6. Aizenberg M.A. Reflection and transmission operators in the transmission problem at plane interface between homogeneous elastic half-spaces. Materials of 41th International Scientific Conference for Students "Student and Scientific-Technical Progress", Mathematics, Differential equations. Novosibirsk State University, Novosibirsk, 2003, 14 (in Russian).

7. Aizenberg M.A. Simulation of interference wave field, single reflected at curvilinear interface between homogeneous media. Materials of 41th International Scientific Conference for Students "Student and Scientific-Technical Progress", Geology, Geophysics. Novosibirsk State University, Novosibirsk, 2003, 16-17 (in Russian).

8. Aizenberg M.A. Reflection and transmission operators in the acoustic transmission problem at plane interface between homogeneous media. Materials of Scientific Conference for Students "Intellectual potential of Siberia". Novosibirsk State University, Novosibirsk, 2003, 3 (in Russian).

9. Aizenberg M.A., Aizenberg A.M. Simulation of interference wave field trace reflected/transmitted by plane interface of two acoustic media. Dynamics of solid media: Scientific Proceeding of Russian Academy of Sciences. Siberian Branch, Institute of Hydrodynamics, 2002, 121, 50-55 (in Russian).

10. Aizenberg A.M., Aizenberg M.A., Helle H.B., Klem-Musatov K.D., Pajchel J. Single Reflection at Curvilinear Interface. Tip Wave Superposition Method with effective reflection coefficient. Open report, E&P Research Centre, Norsk Hydro a.s., Bergen, Norway, 2002.

11. Aizenberg A.M., Helle H.B., Klem-Musatov K.D., Pajchel J. The tip wave superposition method based on the refraction transform. Extended Abstracts, 58th Meeting, European Association of Geoscientists & Engineers, 1996, Paper C001.

12. Aizenberg A.M., Klem-Musatov K.D., Pajchel J., Helle H.B. Seismic simulation by the Tip Wave Superposition method in a complex 3-D model. Open report, E&P Research Centre, Norsk Hydro a.s., Bergen, Norway, 1992.

13. Aki K., Richards P.G. Quantitative Seismology: Theory and Methods. W.H. Freeman, New York, 1980.

14. Alekseev A.S., Kostin V.I., Khaidukov V.G., Cheverda V.A. Recovery of two-dimensional perturbations of the velocity of a vertically inhomogeneous medium from multicoverage data (linearized formulation). Russian Geology and Geophysics, 1997, 38, 12, 2012-2025.

15. Alimov Sh.A., Ilyin V.A. Convergence conditions of spectral representations which respond to self-adjoint extensions of elliptic operators. II. Self-adjoint extension of Laplace operator with arbitrary spectrum. Differential equations, 1971, 7, 5, 851-882 (in Russian).

16. Ben-Menahem A., Singh S.J. Seismic Waves and Sources. New York, Springer-Verlag, 1981.

17. Bleistein N. On the imaging of reflectors in the earth. Geophysics, 1987, 52, 931-942.

18. Brehovskih L.M. Waves in multilayered media. Moscow, Nauka, 1973 (in Russian).

19. Cerveny V., Ravindra R. Theory of seismic head waves. University of Toronto Press, Toronto, 1971.

20. Colton D, Kress R. A direct boundary integral equation method for transmission problems. J. Math. Anal. Appl., 1985, 106, 367-413.

21. Costabel M., Stephan E.P. Integral equations for transmission problems in linear elasticity. Journal of integral equations and applications, 1990, 2, 2, 211-223.

22. DeSanto J.A. Scattering of scalar waves from a rough interface using a single integral equation. Wave Motion, 1983, 5, 125-135.

23. Devaney A.J. & Sherman G.C. Plane-wave representations for scalar wave fields. SIAM Review, 1973, 15, 4, 765-786.

24. Goldin S.V. Estimation of reflection coefficient under migration of converted and monotype waves. Russian Geology and Geophysics, 1992, 33, 4, 76-90.

25. Gray S.H. Seismic imaging. Geophysics, 2001, 66, 15-17.

26. Handbook of Mathematical Functions. Eds Abramowitz M. and Stegun I.A., 1964.

27. Hanyga A., Helle H.B. Synthetic seismograms from generalized ray tracing. Geophys. Prosp., 1995, V. 43, 51-75.

28. Ilyin V.A., Poznyak E.G. Foundations of Mathematical Analysis. Part II. Moscow, Nauka, 1980 (in Russian).

29. Kennett B.L.N. Reflection operator methods for elastic waves. Wave Motion, 1984, 6, 407-429.

30. Kennett B.L.N., Kerry N.J., Woodhouse J.H. Symmetries in the reflection and transmission of elastic waves. Geoph. J. R. astr. Soc., 1978, 52, 215-229.

31. Klem-Musatov K.D., Aizenberg A.M., Helle H.B., Pajchel J. Reflection and transmission at a curvilinear interface in terms of surface integrals. Wave Motion, 2002 (Submitted).

32. Klem-Musatov K.D., Aizenberg A.M., Pajchel J., Helle H.B. Edge and tip diffractions (Theory and Applications in Seismic Prospecting). Lecture notes, University of Bergen, Bergen, 1994.

33. Korn G., Korn T. Mathematical handbook for scientists and engineers Moscow, Nauka, 1977.

34. Landa E. & Keydar S. Seismic monitoring of diffraction images for detection of local heterogeneities. Geophysics, 1998, 63, 3, 1093-1100.

35. Miranda C. Partial Differential Equations of Elliptic Type. New York, Berlin, Springer-Verlag, 1970.

36. Pao Y.-H., Varatharajulu V. Huygens' principle, radiation conditions, and integral formulas for scattering of elastic waves. J. Acoust. Soc. Am., 1976, 59, 6, 1361-1371.

37. Roach G.F. Scattering from unbounded surfaces. Proceedings of Dundee Conference, Pitman Research Notes, 1993, 248-272, Longmans, London.

38. Sen M.K., Frazer L.N. Multifold phase space path integral synthetic seismograms. Geophys. J. Int., 1991, V. 104, 479-487.

39. Treitel S., Lines L. Past, present and future of geophysical inversion – A new millennium analysis. Geophysics, 2001, 66, 21-24.

40. Vladimirov V.S. Equations of Mathematical Physics. Moscow, Nauka, 1971 (in Russian).

41. Wenzel F., Stenzel K.-J., Zimmermann U. Wave propagation in laterally heterogeneous layered media. Geophys. J. Int., 1990, V. 103, 675-684.

42. Weston V.H. Wave splitting and the reflection operator for the wave equation in R^3. J. Math. Phys., 1989, 30, 11, 2545-2562.

43. Zhang Bo. On transmission problems for wave propagation in two locally perturbed half-spaces. Math. Proc. Camb. Phil. Soc., 1994, 115, 3, 545-558.